DeepBionicSyn: Creative 3D Shape Synthesis via Implicit Representation for Organic Biologically Inspired Design

ANONYMOUS AUTHOR(S)
SUBMISSION ID: 671

(a) Input model (b) Synthetic candidates (c) Inspired designs

Fig. 1. DeepBionicSyn takes a collection of natural creations and man-made artifacts as input(a) and synthesizes novel 3D biologically inspired designs(b). Synthetics designs using DeepBionicSyn yield potentially functional and inspiring variations(c).

Biologically inspired design holds great value for product design. Inspired by geometric features from natural creations, designers can create organic nature-inspired shapes. Traditionally, even for experienced designers, biologically inspired design is related with time-consuming or trial-and-error effort. We propose DeepBionicSyn, an approach for automatic creative 3D biologically inspired design. We view the biologically inspired design problem as an out-of-distribution synthesis problem based on a dataset of natural creations and man-made artifacts. DeepBionicSyn is trained on AC-BIONIC, a large-scale dataset containing 28k reference shapes. We mine the required design candidates in a shared neural parametric representation space of the input dataset using a creativity synthetic solver. Finally, a human-in-the-loop local manifold subspace exploration technique allows designers to explore design variants effectively. Compared with previous three-dimensional generative methods for creativity, our framework can meet organic biologically inspired design requirements and does not require pre-analysis for shape collections. We evaluate the effectiveness of our method on a chair product biologically inspired design task based on the chair-animal hybrid dataset. We introduce a metric for evaluating creative biologically inspired design tasks to quantitatively assess our approach and other potential alternatives.

CCS Concepts: • **Computing methodologies** → **Computer graphics**; • **Applied computing** → **Arts and humanities**; • **Human-centered computing** → Systems and tools for interaction design.

0730-0301/2023/3-ART $15.00
https://doi.org/10.1145/nnnnnnn.nnnnnnn

Additional Key Words and Phrases: implicit representation,biologically inspired design ,shape synthesis, deep geometry learning

ACM Reference Format:
Anonymous Author(s). 2023. DeepBionicSyn: Creative 3D Shape Synthesis via Implicit Representation for Organic Biologically Inspired Design. *ACM Trans. Graph.* 1, 1 (March 2023), 19 pages. https://doi.org/10.1145/nnnnnnn.nnnnnnn

1 INTRODUCTION

Biologically inspired design (also called bionic design) is one of the key trends in product design. In this paper, we limit the topic to form-wise biologically inspired design, which has received increasing attention from the product design community. Typically, in biologically inspired design, product functions and nature-inspired forms are blended into mechanical structures, microscopic materials, or forms to optimize the outcome of the product. Unlike bio-inspired design based on mechanical structures and microscopic materials, form-wise biologically inspired design can be used to create amazing artistic effects in an abstract and organic form by combining abstract features of natural creations with man-made artifacts [Holt et al. 2005]. For example, animal chairs (see Figure 2) serve as an enjoyable and sustainable product that can be used in children's education and as public sculptures.

However, organic biologically inspired design breakthrough is costly. Off-the-shelf nature-inspired 3D models of man-made artifacts are rare due to the *synthetic challenge* and the *modeling challenge*. The *synthetic challenge*: Initial inspiration is usually found through trial and error by repeatedly extracting, analyzing, and

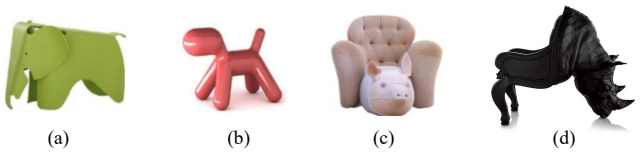

Fig. 2. Examples of biologically inspired product designs. (a) A children elephant chair from Charles Eames 2017. (b) An animal chair in organic form from Eero Arinio 2003. (c) An armchair in the shape of pig generated from text-prompt generator [Ramesh et al. 2021]. (d) A concrete rhinoceros biologically inspired chair from Maximo Riera 2020.

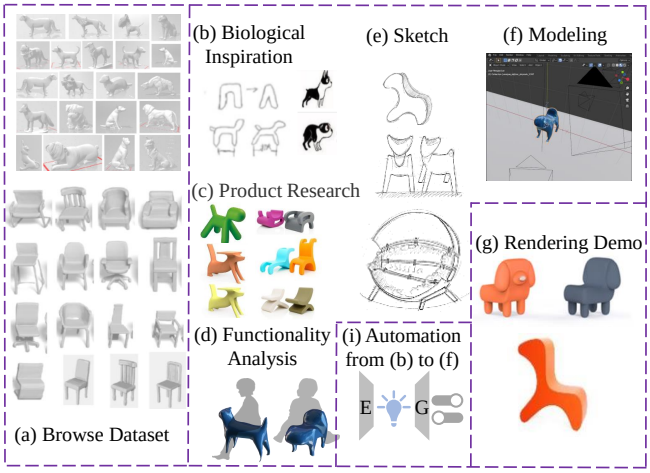

Fig. 3. The traditional process of creative shape biologically inspired design: Designers browse shape samples of natural creations, man-made artifacts (a) and similar products (c). Then designers analyze biological features (b) as inspiration set and functionality of object product as design target (d). Before creating 3D assert, they developed product plans in the form of sketches. (e). Finally, models are built in 3D software (f) and rendered (g). Our approach takes 3D models from (a) as input and automates the procedure of b-f (I).

blending features of biologically inspired objects (e.g., man-made artifacts) and the design target (e.g., natural creations). These inspirations culminated in a sketch that was used to guide the model (see Figure 3 b-c). This step relies heavily on a stroke of inspiration and the prior knowledge of a professional designer. It has a decisive influence on the final product result. The *modeling challenge*: Modeling efforts are required for reconstruction from the sketch to the 3D geometry prototype (see Figure 3 e-g). It is challenging to ensure that the final biologically inspired shape meets abstract and organic style requirements. In particular, in Figure 2, *Eero Arinio 2003* is more in line with the organic abstraction of the form. *Charles Eames 2017* is focused on the texture of imagery rather than the geometric shape and *Maximo Rlera 2020* is figurative. Our work focuses on solving the *modeling challenge* and *synthetic challenge* in the biologically inspired shape design process.

There are currently gaps in the literature with respect to addressing the two challenges mentioned above. Previous computational biologically inspired design methods[Yu et al. 2019] have been limited to graphic contour design. In the graphics community, one of the mainstream ideas to solve the *synthetic challenge* is to segment two types of objects and then assemble the components[Chaudhuri et al. 2013; Chaudhuri and Koltun 2010; Xu et al. 2012]. However, these methods do not take the abstraction and simplification of shapes into account, resulting in the inability to form seam-free combinations and organic forms [Holt et al. 2005] for artistic design effects. Furthermore, task-specific rules, such as presegmentation [Duncan et al. 2015; Huang et al. 2017] or shape grammar [Guo et al. 2014] are needed. In contrast, it is possible to obtain organic 3D synthetics in a task-independent manner through interpolation in latent space [Chen and Zhang 2019; Wu et al. 2016], especially with implicit representation [Chen and Zhang 2019; Mescheder et al. 2019; Park et al. 2019]. However, the off-the-shelf generative model suffers from low-fidelity when fusing cross-category shapes in a biologically inspired design[Schor et al. 2019].

We analyzed this issue and gained two insights. On the one hand, employing an off-the-shelf implicit representation model is sufficient to meet the abstract and organic demands for the *modeling challenge*. The key is to further mine the generative model knowledge, namely, a subset of latent codes. We consider a multi-category and creative synthesis problem as a variant of the out-of-distribution (OOD) generation problem. We hope to obtain a multimodal OOD distribution (see Figure 8 (d)) given input training dataset distributions. Then, the candidate set is obtained by sampling from the OOD distribution. On the other hand, synthetics of high fidelity and biologically inspired value should be controlled by the users themselves as a human-in-the-loop process, in addition to relying on rule-based latent space mining. Our approach should help designers explore candidate shape collections and find the desired variants on the basis of selected candidates. The OOD generation problem can also be solved considering the human-in-the-loop approach. Inspired by interpretable directions [Chiu et al. 2020; Härkönen et al. 2020; Shen and Zhou 2021], desired variants are obtained by exploring generator knowledge via local manifold search [Chiu et al. 2020].

Based on this, we introduce implicit autoencoder (IMAE) [Chen and Zhang 2019] as a parameterization representation and propose a creativity synthetic solver. The core idea is to constrain the discovery of synthetics with biologically inspired value as an optimization problem in the OOD area, according to the hybrid score function, to obtain the top K candidates. Then, we provide an interface to help the user explore candidate distribution and potential variations in manifold subspace by changing semantic slides. In the experiments, we use the animal-chair design as an example. Since there are no research studies that can be directly applied to the task at hand, we quantitatively provide a method to evaluate the quality of bioinspired design generators. The baseline includes existing overall potential alternatives and alternatives to creativity synthetic solver. In addition, to demonstrate the effectiveness of our system design, we measure the efficiency of our overall system through several case studies. The results show that our system can be used to address the three main needs of designers and outperform the baseline in terms of quantitative evaluation results and qualitative designer satisfaction.

Our work makes the following contributions:

- We propose a novel task for learning-based creative 3D biologically inspired design. The task, from the perspective of a deep generative model, is different in terms of the final result and the challenges faced compared to the tasks solved by previous assembly-based approaches.
- We theoretically and quantitatively demonstrate that creativity and biologically inspired designs are highly relevant to out-of-distribution synthesis. We consequently propose a proper shape synthesis framework as a creativity synthetic solver.
- We present a bistage hybrid synthetics computational system. It not only prevents users from getting bored with the infinite number of candidates generated by the shape generator but also provides enough freedom to explore the design variants in a high-level manner.

2 RELATED WORK

Biologically inspired design. Fields of research such as "biological-inspired design", "bionics", "robotics", and "biomimetics" originated during the mid-twentieth century and are now widely explored fields. More recent bio-design, mainly developed in Architecture, has defined as "biophilic design"[Kellert et al. 2011] to describe an "innovative approach that emphasizes the necessity of maintaining, enhancing and restoring the beneficial experience of nature in the built environment." biologically inspired design is classified in terms of form, function, and system [Bertolini et al. 2006]. In this paper, creative biologically inspired shape design emphasis on a form-wise manner, combining abstract features of nature creations with man-made artifacts [Holt et al. 2005]. Previous computational biologically inspired design methods [Yu et al. 2019] are limited to 2D form. In the more general design community, the generative design of both rule-based approaches [Attar et al. 2010; Matejka et al. 2018] in 3D and deep generative model (GDM)-based approaches [Oh et al. 2019] in 2D was proposed. Rule-based generative design is difficult to accommodate the diversity required for biologically inspired. 3D generative design [Bidgoli and Veloso 2019; Shu et al. 2020] is closer to our work but the field mainly focuses on single-category synthesis. The design community is also considering increasing the diversity of generative design by changing the loss [Chen and Ahmed 2020; Elgammal et al. 2017]

Data-driven geometry modeling. In the graphics community, the evolving field of data-driven geometry modeling provides ideas for solving biologically inspired design problems. With only a few data references, a large number of various 3D shapes are synthesized [Kalogerakis et al. 2012]. Then, a human-in-the-loop interaction interface allows users to explore shape collections [Averkiou et al. 2014; Marks et al. 1997] or to further edit [Chiu et al. 2020; Yang et al. 2021]. This pipeline partly covers the *modeling challenge* and the *synthetic challenge*.

However, regarding the *synthetic challenge*, biologically inspired design shall not simply mimic the training set distribution but rather a blend of natural creation and man-made artifacts. It remains a challenging problem to automatically generate biologically inspired designs bridging the functionality of man-made artifacts and the biologically inspired morphological values of natural creations. One of the mainstream ideas to solve the *synthetic challenge* is to segment the two types of objects and then assemble the components [Chaudhuri et al. 2013; Chaudhuri and Koltun 2010; Xu et al. 2012]. The work that most closely resembles our goal is *zoomorphic design* [Duncan et al. 2015], which uses a rule-based approach to assemble man-made artifacts and animals in an energy minimizing manner. However, assembly-based methods ignore abstraction and simplification of shapes, resulting in the inability to form seam-free combinations and organic forms [Holt et al. 2005] for artistic design effects. In addition, some prior expert knowledge is required, such as presegmentation [Chaudhuri et al. 2013; Xu et al. 2012] or shape grammar [Guo et al. 2014]. To date, some studies have found it possible to obtain smooth 3D synthetics through interpolation in latent space [Chen and Zhang 2019; Wu et al. 2016], especially with a fine parametric representation such as a deep implicit representation [Chen and Zhang 2019; Mescheder et al. 2019; Park et al. 2019]. They still mimic the training set distribution. Therefore, an off-the-shelf implicit generative model is more suitable for the *modeling challenge*, leaving the *synthetic challenge* to be solved. A straightforward idea for out of distribution synthesis (OODS) problem is to add loss to encourage diversity and different synthetics from training dataset[Elhoseiny and Elfeki 2019; Sbai et al. 2018]. An interesting finding is that the quality of samples obtained at the edge of the training data distribution is higher than those very far from the training data distribution[Elhoseiny and Elfeki 2019]. This means that we need to further explore the latent space of the generative model to target valuable OOD regions.

3D shape style transfer [Chen et al. 2021; Yifan et al. 2020] seems to be a feasible alternative. However, we found that biologically inspired design is not a global and local synthesis problem. We confirm this suspicion by a set of baseline comparison experiments.

Latent space exploration. Discovering synthetics to meet demand from pre-trained latent variable generative models is an important part of Artificial Intelligence Generated Content(AIGC). Although AIGC offers an unlimited number of synthetics, AIGC easily transforms a trail-and-error manual content creation process into a tedious selection from a large number of candidates. As a result, there is a growing interest in providing an appropriate set of interactions for generative models[Yue et al. 2021]. A pioneering work from a user interface point of view is the Design Galleries[Marks et al. 1997]. They provide a projector for browsing a set of samples based on their embedding in parametric representation space. Averkiou extend the projector to 3D shape gallery[Averkiou et al. 2014]. In addition, a 3D interactive fine-tuning tool such as the one designed by umetani[Umetani 2017] is also necessary. Umetani's tool is based on latent space of generative model but the control is too low-level and lack of diversity. Recent research in the field of image synthesis aims at shifting synthetics distribution from the original dataset distribution, such as truncation trick [Karras et al. 2019], and interpolation in latent space for pretrained model. Furthermore, exploring interpretable direction (EID) [Shen et al. 2020b; Xia et al. 2021] for transforming synthetics along a high fidelity trace but actually towards out-of-training-dataset distribution. From this perspective, interpolation or morphing method [Dosovitskiy et al.

2015] is taken as a special case of data-specific EID. EIDs can be found by a supervised approach [Shen et al. 2020b]. There are also a number of unsupervised approaches that use pre-trained generator weights [Chiu et al. 2020; Shen and Zhou 2021] or the feature space distribution [Wang et al. 2021] of the training set to obtain the corresponding interpretable directions. We find the local manifold subspace search approach [Shen and Zhou 2021] suitable to explore the design variants with high-level semantic change.

3 OVERVIEW

The 3D shape biologically inspired design task is inspired by the 3D shape synthesis problem, and mathematics modeling will be introduced first. Then, an overview of the biologically inspired design synthesis framework is presented in Figure 4.

Problem formulation. In three dimensional data space $\mathcal{X}$, given *man-made artifacts* samples $\mathcal{D}_d = \{x_k\}_{k=1}^{M}$ and *natural creations* samples $\mathcal{D}_b = \{x_k\}_{k=1}^{N}$ following probability distribution of $p(d)$ and $p(b)$ respectively, our goal is to search for 3D shapes of high fidelity and high biologically inspired value that incorporate semantic features from the input shape collections. From the representation learning perspective, we should project high-dimensional 3D data into a learned joint compressed parametric representation space $\mathcal{Z}$ with encoder $E : \mathcal{X} \mapsto \mathcal{Z}$, a low-dimensional Euclidean space. We suppose embedding of distribution as $p(z_d)$ and $p(z_b)$. Then, we choose a specific sampling strategy to find a latent code sequence $\{z_k\}_{k=1}^{Y} \subset Z$ of ideal biologically inspired design distribution $p(z_k)$. Finally, a generator $G : \mathcal{Z} \mapsto \mathcal{X}$ maps latent code sequence$\{z_k\}_{k=1}^{Y} \subset Z_I$ to 3D data as a creative biologically inspired design shape.

Challenges. According to the traditional process of creative shape biologically inspired 3, the challenges can be categorized as the *modeling challenge* and *synthetic challenge*. The *modeling challenge* means that finial synthetics should be sufficiently functional, organic and abstract. Compared to the assembly-based 3D shape representation from fit-and-diverse [Xu et al. 2012], implicit deep generative models provide a smooth representation space, allowing for certain abstractions and organic forms. However, even for off-the-shelf generative models, this problem is still nontrivial, as sampling from the low probability density area of the dataset (OOD area) required for biologically inspired design suffers from low fidelity problems. The problem is related to the *synthetic challenge*. The *synthetic challenge* is a core problem for creative biologically inspired design. Synthetics should refer to the features of different categories of input shapes and maintain a large diversity to meet the needs of designers. To make matters worse, for generative models, if a data-driven approach requires sufficiently similar data for training, the biologically inspired design requires a zero-sample approach, that is, forcing the generative model to generate samples that do not match the original input data distribution. We refer to this challenge as the out-of-distribution synthesis (OODS) problem. In OODS, there is an extreme scarcity of datasets and synthetics have low fidelity. Finally, this study, as a general computational biologically inspired design framework, should be category-independent and task-agnostic.

Methodology. To maintain the fidelity and diversity of synthetics, an AC-BIONIC dataset with design-oriented (D-O) and performance-oriented (P-O) data enhancements (see 4 a) was created, containing over 20k weak-shot labeled 3D geometry data with natural creations and man-made artifacts for input, as well as manual biologically inspired designs for the out-of-distribution validation test. Inspired by the traditional process of creative shape biologically inspired design in Figure 3, we propose a bistage approach. First, we use an implicit generative model to learn a parametric representation of the dataset. We limit potential biologically inspired design exploration space to the OOD area of this representation space, which will theoretically and experimentally tested. Second, a high lack of diversity and low fidelity synthetics would lead to selection difficulties due to an improper sampling strategy. Infinite candidates convert the original time-consuming trial-and-error modeling effort into another tedious selection effort. To avoid this situation, we use a creativity synthetic solverto determine out a batch of candidates $\{G(x_i)\}_{i=1}^{M}$ and enable users to explore and further fine-tune candidates. The cold start module begins with a sampling strategy from latent space $\mathcal{Z}$ with a heuristic hybrid objective function$f : \mathcal{X} \mapsto \mathbb{R}$ to find latent code sets(see Figure 4 c), where filtered out synthetics have high fidelity and high biologically inspired value (equivalence to high OOD score). Then, we design an interface, where the user can interact with the system, select ideal synthetics and fine-tune results with several semantic directions. Finally, postprocess is performed to ensure low-poly and minimalist meshes as the final organic biologically inspired design (see Figure 4 d).

4 DATASET OF DEEPBIONICSYN

We created the AC-BIONIC dataset, which combines an animal-chair dataset, as the input natural creations and man-made artifacts, and a set of creative synthetics with semantic annotations or the designer's manual biologically inspired design independent of our model. It is hoped that the dataset will be used to accelerate relevant research on automated creative biologically inspired design and the recognition of creative assets from outside-of-distribution synthesis.

Data collection. We collected over 20k training data points for unsupervised generation tasks. There are 6778 chairs from the ShapeNet dataset [Chang et al. 2015] and 132 various animals collected from the online 3D model store at our own expense. The design faculty and students used a self-developed web application to screen potential products that met the demand of biologically inspired design and were considered of value for creative inspiration. Potential copyright issues in animal datasets were avoided by eliminating privacy. 100 augmented designer's manual biologically inspired design is provided for both *modeling challenge* and *synthetic challenge*. In *modeling challenge*, designers modeled based on existing biologically inspired design images collected from well-known works. In *synthetic challenge*, designers was advised to browse the shape collection of training dataset and try to create the coarse geometry models.

Data augmentations. To address the lack of ground truth for 3D bio-inspired design and the unbalanced distribution of the two kinds of 3D models, a widely used strategy is data augmentations. In

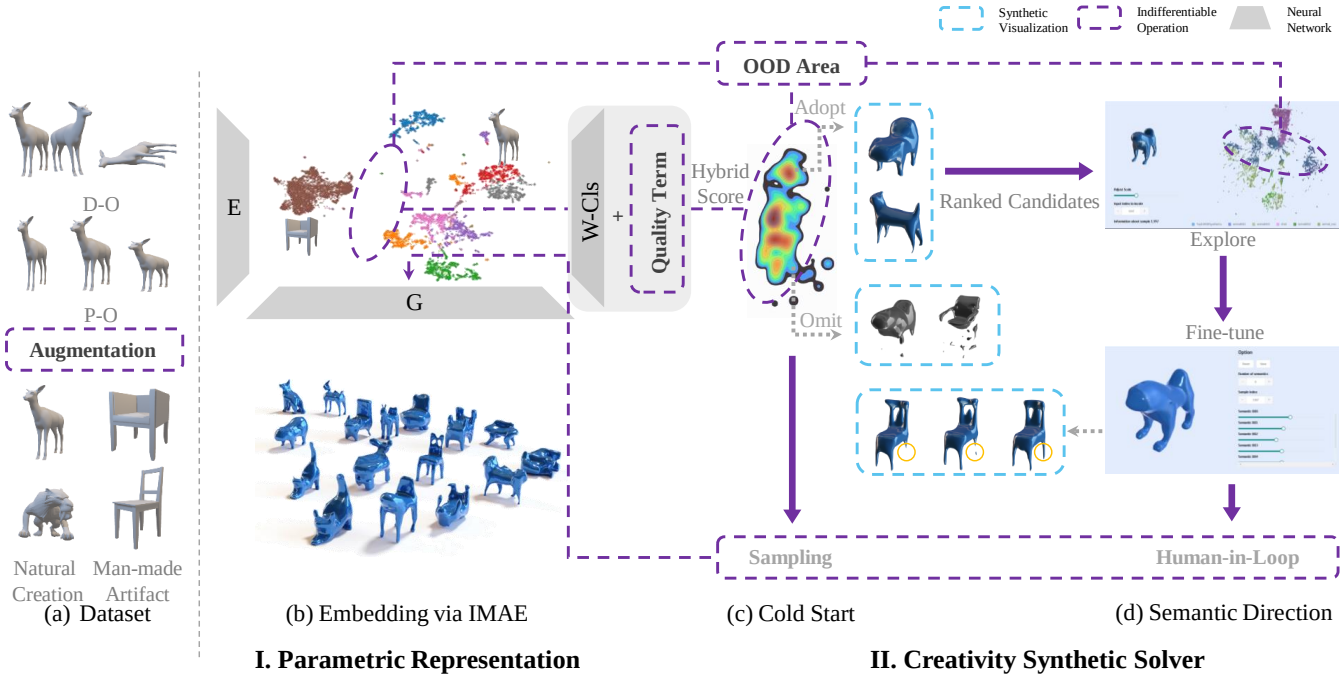

Fig. 4. Overview of our framework for 3D biologically inspired design, which combines deep implicit generative modeling and user-in-the-loop interactive. (a) Dataset consist of natural creations as inspiration and man-made artifacts as product target. (b) After training an IMAE, there exist some biologically inspired synthetics in the shape perception boundary in latent space. The trained encoder and decoder form a parametric **representation** of 3D shape. In latent space, a problem is how to find out creative biologically inspired design. **Creativity Synthetic Solver** obtains final results via two steps. (c) A hybrid function containing weak-shot classifiers(W-Cls) and quality term is deployed to get high score candidates. Through multimodal optimization sampling, candidates filtered out are recommended to users as if cold start in recommendation. (d) Candidates with high scores are then inputted into a human-in-loop system. The Projector view of the web interface allows the user to explore the entire design space. After selecting the desired synthetic, a local manifold subspace search algorithm is employed to explore potential design variants in a slide-bar manner.

the biologically inspired design synthesis task, data augmentation methods are divided into design-oriented (D-O) and performance-oriented (P-O) methods. The use of them both expanded the size of the training animal dataset from 132 to 13,804.

D-O data augmentation focuses on the transfer of design knowledge to the preparation of data sets for design requirements. For example, the combination of shapes in different orientations counts as a factor in a designer's design process. After evaluating existing biologically inspired products and brainstorming, generative designs that considered multiple directions allowed us to explore additional possibilities. Considering the symmetry of the target product and the trade-off between diversity and efficiency, we chose to apply a rotational transformation of the natural creation dataset in seven directions to achieve a diverse blend of syntheses.

P-O data enhancement aims to improve the performance of deep generative models. Generators suffer from unbalanced training data, especially with only hundreds of animal datasets. Nonrigid deformation, such as affine transformation, is an effective approach to alleviate this problem. We warp the training dataset on three orthogonal axes with various degrees.

In addition to the two data augmentation techniques already mentioned, animal motion augmentation [Zuffi et al. 2017] and assembly [Guo et al. 2014] augmentation seem to also be available. However, we do not take them into account since we hope that our approach is not limited to specific tasks as mentioned in the category-independent hypothesis. Both methods require corresponding domain knowledge. For example, SMAL [Zuffi et al. 2017] cannot be directly applied to birds or more strange monsters. In contrast, P-O and D-O augmentation are task-agnostic.

Representation. Following IMAE [Chen and Zhang 2019], we represent the 3D model as mesh, voxel, point-value pair, and embedding vectors. A set of toolkits enable users to input a mesh file and obtain other data formats used in the whole pipeline. More details on the data transformation are shown in Figure 5.

5 OUT-OF-DISTRIBUTION SYNTHESIS PROBLEM

The *synthetic challenge* poses a challenge for deep generative models, which tend to produce designs that are similar to those in the training data, rather than novel or creative designs [Chen and Ahmed 2020; Schor et al. 2019]. This limitation makes it difficult to use these models for creative biologically inspired shape design in the *synthetic challenge*. To address this challenge, we propose to treat it as an Out-of-Distribution Synthesis (OODS) problem, where the

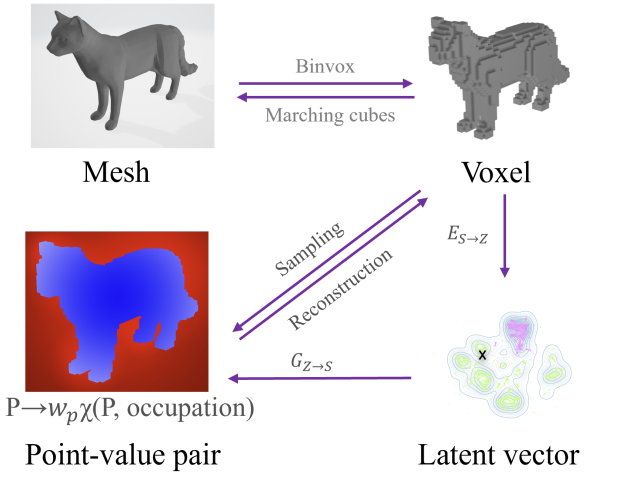

Fig. 5. Data representation and transform methods: The mesh shapes were converted to 64^3 voxel via binvox toolkit[Nooruddin and Turk 2003]. Point-value point is similar to point cloud, serving as the middle process of training. The sampling method[Chen and Zhang 2019] is surfaces-near and for progressive training. Latent vector is our desired parametric representation.

goal is to generate novel biologically inspired synthetics. This is distinct from the general generative task, which focuses on fitting the prior distribution to the training data distribution, whereas OODS emphasizes fitting the prior distribution to different distributions and meeting the requirements of the application domain. The target distribution depends on the objective function that is designed for the task.

5.1 Creativity existence hypothesis

We propose to construct an axiomatic system for creative biologically inspired design, which will provide a mathematical framework for defining and evaluating designs in this domain.

Definition. To give further insight into biologically inspired design, some basic conceptions will be presented.

- *Natural creations* and *man-made artifacts*. The creative biologically inspired design task involves two main categories: natural creations and man-made artifacts. This does not mean that our framework is limited to only these two categories of data. For example, in the case of the animal chair, the natural creations category may include a wide range of animal shapes and species, including mythical creatures such as Pegasus.
- *High fidelity*. We will evaluate the fidelity of synthetics using metrics such as smoothness and connected component counts, to ensure that they are visually coherent and well-formed. This definition ensures that the synthetics are both abstract and functional, and meet the desired criteria for creativity and realism.
- *Out-of-distribution area*. The out-of-distribution area is defined as a set of points in the probability space that have a probability lower than a given threshold. In mathematical terms, this means that given a probability space $(\Omega, \mathcal{F}, P)$ and a threshold $0 < M < 1$, the sufficient and necessary condition for an open set $A \subset \Omega$ to be an out-of-distribution area is that for any $z \in A$, we have $p(z) < M$..

Hypothesis. Our computational framework for biologically inspired design is based on three hypotheses. The first two hypotheses are inspired by the designer's design process, as shown in Figure 3. The third hypothesis is empirical, and is derived from observations of existing generative models and tasks.

- *Category-independent hypothesis*. Because the categories of natural creations and man-made artifacts are coarse-grained, our framework for biologically inspired design will not consider category-specific methods. For example, there are supervised semantic segmentation and functional detection methods that are useful for improving the quality of generated objects in the categories of chairs or animals, but they may not work in a brand-new category such as aliens [Xu et al. 2012]. The training dataset will be labeled only with the general categories of natural creations and man-made artifacts, and will be processed using methods that are useful for these two coarse-grained categories.
- *Fusion hypothesis*. Synthetics with *high biologically inspired value* are a balance between *Natural creations* and *man-made artifacts* distributions, rather than being based solely on the in-distribution of reference objects. Our framework attempts to combine biological properties with product semantics, to create designs that are both functional and creative. This combination of features results in synthetics that fall into the out-of-distribution area in the shape semantic space, and can be learned by deep generative models as a latent representation.
- *Existence of the high-fidelity hypothesis*. A sample of high fidelity is a subset of the training dataset that falls into the region of low probability. This hypothesis is based on empirical observations and has been demonstrated in experiments (see Figure 16). In other words, we expect that high-fidelity samples will be rare or unusual within the training dataset, and will require the generative model to explore and generate novel or creative designs.

Finally, we propose a theorem that demonstrates that our goal of creating creative biologically inspired designs is possible. This theorem shows that the desired synthetics can be found in the out-of-distribution area, by searching for high-fidelity samples. The proof of the theorem is provided in the appendix.

Heterogeneous distribution lemma: In creative bionic design tasks, natural creations have a different distribution from man-made artifacts in latent space $\mathcal{Z}$.

Existence of the out-of-distribution area lemma: In a latent space $\mathcal{Z}$, there is at least one *out-of-distribution area*.

Creativity existence theorem. In the low probability of training dataset distribution for creative biologically inspired design, there exist high fidelity objects, and they follow *fusion hypothesis*. We define them as *creative synthetic*.

And then, we can infer that general generation tasks cannot solve creative biologically inspired design tasks because the general generation task violates *the heterogeneous distribution lemma*, the

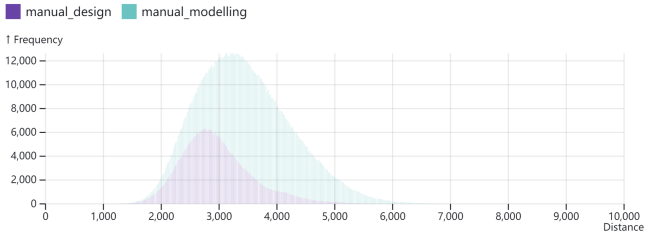

Fig. 6. Distribution of one-by-one chamfer distances between manual bio-inspired shapes and reference datasets.

prerequisites of the *creativity existence theorem*. To achieve creative biologically inspired design, we should introduce a new generative framework to generate creative synthetics. 3D shape generative model can be used to learn a proper parametric representation space $\mathcal{Z}$. Then, a sampling algorithm is required to filter out creative synthetics. The scoring function aims to identify synthetics of *high-fidelity* and *high biologically inspired value*. The former can refer to the *high-fidelity* definition and *fusion hypothesis*, while the latter has to take into account the human goodness function. The user interface will be an option to recommend *creative synthetics* and allow users to explore the design space freely.

5.2 Out-of-distribution test

The out-of-distribution test is used to demonstrate that for a pre-trained parametric representation network, the majority of biologically inspired designs designed by human designers fall in the OOD area. We prepared 50 *manual modelling* from existing reconstructions of well-known bio-inspired designs, as well as *manual design* independently created by designers browsing our dataset. And then, we computed chamfer distance (CD) between them and training data in our AC-BIONIC dataset. The results (see Figure 6) illustrate that the distributions of the bio-inspired designs are far from their reference data. *Manual modelling* and *manual design* distributions are close and both fall into the OOD area.

The engineered implementation of OOD Area is to introduce an auxiliary weak-shot classifier (W-Cls) into the latent space. An intuitive way to understand this is that when the network has difficulty determining which class of the input data set the generator corresponds to, then the generator is naturally far away from the high density area of the training set data distribution. More details of this indicator are given in Equation 7.

6 BI-STAGE CREATIVE BIOLOGICALLY INSPIRED DESIGN SYNTHESIS

To solve the Out-of-distribution synthesis (OODS) problem, we disentangle the solution into a parametric representation and the creativity synthetic solver. We consider a bio-inspired-specific method that trades off the shifting distribution and fidelity to natural creations and artifacts inspired by interpolation blending. And then we introduce an unsupervised EID method for further human-in-loop editing.

6.1 Implicit deep generative model

modeling challenge is to obtain a smooth and semantically meaningful parametric representation of the 3D data owing to biologically inspired design demands for abstract and organic forms. IM-GAN [Chen and Zhang 2019], composed of a 3D CNN encoder, an implicit decoder and a vanilla latent-GAN [Achlioptas et al. 2018], successfully produces smooth shape morphing effects. We adopt it in our work to achieve smooth parametric representation.

Implicit representation is actually is the signed distance field $F()$. For every input point p, $F(p) = \chi(P, occupation)$. χ is the characteristic function mapping $\mathbb{X}$ to $\{0, 1\}$, and $occupation$ indicates the states in which the point P is inside the 3D shape model. If P meets $occupation$ then $F(p) = 1$. The implicit decoder utilizes the fact that the MLP neural network $f_\theta()$ is good at fitting isosurface [Chen and Zhang 2019], a continuous boundary of query points P. The loss function is as follows:

$$L(S;\theta) = \frac{\sum_{p\in S} |f_\theta(p) - F(p)|^2 \cdot w_p}{\sum_{p\in S} w_p}, \tag{1}$$

where w_p is the sampling weight and the inverse of the sampling density points near the point p. f_θ is an implicit-decoder. After unsupervised training, we achieve a parametric representation $\mathbb{Z} \subset \mathbb{R}^n$, the whole point set of $F(p), \forall p \in \mathbb{X}$.

6.2 Failure modes for in-distribution generative models

We can apply following usual method to explore the latent space and attempt to mine creative samples(Figure 8). However, if we directly apply off-the-shelf 3D shape generative models [Chen and Zhang 2019] to *creative biologically inspired design synthesis* task, or explore the potential space with mainstream methods[Achlioptas et al. 2018; Wu et al. 2016], we will realize two failure modes. These challenges are the out of distribution synthesis and feature degradation.

Before introducing the two problems, let us introduce the commonly used methods for exploring the latent space(see Figure 7 b and c). They can be divided into three categories: random sampling, linear combinations based on selection vectors, and direction manipulation. Detailed descriptions are included in the appendix. In practice, they are difficult to accomplish our tasks directly due to following challenge:

Out of distribution synthesis. In-distribution synthesis, generating within the dataset distribution, brings two potential drawbacks, one is the synthetics category bias and the other is the fragmentation problem. The former violate *fusion hypothesis*. For example, latent-GAN [Achlioptas et al. 2018] solved the in-distribution generation problem. It is suitable for the natural creations or man-made artifact categories. Therefore, in the creative biologically inspired design the latent-GAN may be not proper. The latter is empirical, i.e., when the network tries to generate new samples in regions of sparse training data, the synthetics will behave in a broken way. This phenomenon requires us to explore a new deep generative framework for out-of-distribution synthesis problem. The framework should ensure high fidelity and more biologically inspired synthetics.

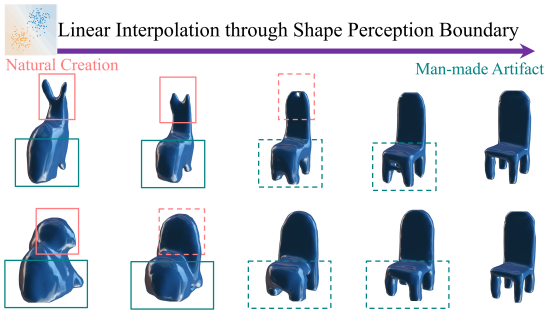

Fig. 7. Feature degradation problem occurs during simply interpolation. During the interpolation from animals to chairs, note that biological features(solid line) of head(orange), leg(red) and tail(green) are fading away during interpolation.

Feature Degradation. Feature degeneration(Figure 7) means that some detailed form-wise features disappear during latent code transformation (e.g., interpolation). This issue limits the further application of deep generative models to mine potential creative samples. A straightforward solution is to deploy a feature detector to identify the semantic features of the shape of both. However, the method violates the *category-independent hypothesis* unless there is an unsupervised feature detector. Note that the label is weak-shot, only containing natural creations, man-made artifacts. Therefore, the feature-preserving interpretable direction from a high-fidelity initial point is suitable to explore the feature blend results and recover the potential feature degeneration.

Two challenges inspired us to design a bi-stage approach, a creativity synthetics solver to solve *synthetic challenge* and *modeling challenge*.

6.3 Creativity synthetics solver

Since it has learned an implicit representation space for the occupation field of a latent creative biologically inspired design collection, a high lack of diversity and low fidelity synthetics would lead to selection difficulties due to improper sampling strategy. It converts the original time-consuming trial-and-error modeling effort into another tedious selection effort. To avoid this *synthetic challenge*, it requires an interface to display Projected initial candidates from *Cold Start Recommendation* and a local manifold exploration strategy to allow human-in-the-loop fine-tune for potential design variants.

6.3.1 Cold Start Recommendation. To address the low-fidelity issue in the out-of-distribution (OOD) region, we propose to transform the given training dataset distribution into a cold start distribution. Similar to the *cold start problem* in recommendation tasks, our framework requires an efficient strategy for extracting the first batch of samples $G(z_i)_{i=1}^{M}$ from the latent space $\mathcal{Z}$ with high fidelity and large diversity for the initial user interface. To address this challenge, our approach involves two components: (1) a heuristic scoring function for evaluating the *creative biologically inspired synthetics* of *high fidelity* and *of high biologically inspired value*, and (2) an efficient sampling method for the latent space that focuses on high-scoring

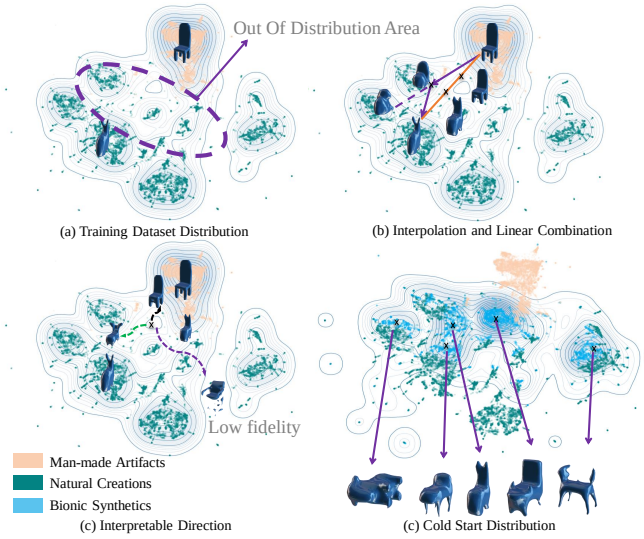

Fig. 8. Motivation of cold start method: Given various natural creatures(green scatter) and man-made artifacts(pink scatter) in latent space. We hope to compute a multi-modal cold start distribution, where each peak representing a potential category of biologically inspired design. The contour represents the density of training dataset(a). The gap between man-made artifacts and natural creation is described as out-of-distribution(OOD) area.

synthetics. Therefore, we design an optimization strategy referring with a heuristic hybrid objective function $f : \mathcal{X} \mapsto \mathbb{R}$.

Previous latent space exploration methods such as **interpolations** and **arithmetic** produce samples based on manual sample selection(see Figure 8 b). In fact, they are linear combinations to explore the OOD region, relying on a few samples as a vector base. If we consider the local manifold of one point, there are several interpretable directions (see Figure 8 c) to explore potential changes locally. However, they will face low-fidelity challenge. For the low-fidelity issue in the OOD area, most of them may give the point to a broken appearance. To encourage the synthetics to fall in the OOD region and retain high fidelity, *we attempt to transform a given training dataset distribution into a cold start distribution*(see Figure 8 d). Probability density is related to fidelity and biologically inspired value via a heuristic hybrid score function.

Hybrid scoring function. Since desired synthetics are the trade-off of biologically inspired value and fidelity, the hybrid objective function consists of a connected component counts function as *quality term* and a fully-connected binary classifier as *W-Cls* to distinguish design targets from biologically inspired references. The effect of hybrid scoring function is shown in Figure9 Connected component counting functions make the objective function $f(x)$ a **black-box**, that is, it is unknown to general closed-form or differential information. The connected component number of a latent vector z can be obtained by discretizing the occupation fields of synthetics $G(z)$:

$$N_{cg}(z) = \phi_{cc}(\{p | f_\theta(z, p) > \delta, \forall p \in \{[0, N_r] \cap \mathbb{Z}\}^3\}) \quad (2)$$

where δ is the threshold to discretize the continuous occupation field.N_r is the object resolution of a voxel. $f_\theta(z, p)$ is the implicit occupation field in query point p, ϕ_{cc} is connected component number function mapping voxel to $\mathcal{R}$.

Although ϕ_{cc} is highly black-box and not differentiable, we still find an differentiable approximate upper bound $\hat{\phi}_{cc}$ directly encourage the lower number of connected components for synthetics during training. We first transform sampled points set p as graph $G = (V, E)$. The graph is extracted from a grid with sampling resolution 64^3. Vertex V is valued with occupation fields in target point and The edge $E = e_{ij}$ indicates whether two vertex are adjacent to each other. According to Euler's formula of Single Connected Diagram, we have $V - E + F = C + 1$, where F represents face number and C is our target, connected components number. Given input shape x, we construct a differentiable approximation function for C as $R(X)$:

$$R(V) := |V| - |E| = \sum_i F(v_i) - \sum_i \sum_{j \in \Omega(i)} \frac{F(v_i)F(v_j)}{2} + |k|, \quad (3)$$

where $F(v_i) \in \{0, 1\}$ respects to whether the point of vertex v_i is occupied. $\Omega(i)$ represents the neighbor 26 vertexes of given vertex v_i. The number of e_{ij} is computed by $F(v_i)F(v_j)$ since it will equal to zero if one of v_i and v_j is not occupied, which is easily achieved with one layer of convolution. $|k|$ is a constant. Then we discretize the schematic function $F(v_i)$ into a differentiable bounded $f(v_i) = \frac{1}{\sqrt{2}\sigma} e^{-\frac{x^2}{2\sigma^2}}$, since IMAE outputs continuous values from 0 to 1. Finally, we have a term $R(V)$ encouraging low number of connected components:

$$R(V) = \sum_i f(v_i) - \sum_i \sum_{j \in \Omega(i)} \frac{f(v_i)f(v_j)}{2}. \quad (4)$$

Since a differential loss function, we retrain our IMAE model for better quality of synthetics with loss as following:

$$L(S; \theta) = \frac{\sum_{p \in S} |f_\theta(p) - F(p)|^2 \cdot w_p + R(f_\theta(p)) \cdot w_p}{\sum_{p \in S} w_p}. \quad (5)$$

Given the embedding of man-made artifacts $\mathcal{D}_{zd} = \{z_k^d\}_{k=1}^M$ and natural creations $\mathcal{D}_{zb} = \{z_k^b\}_{k=1}^M$. A weakshot classifier(W-Cls) $f_c(z) = \text{argmax}_i P(Y = i|z)$ is trained with the binary classification entropy loss:

$$L(\theta) = \sum_i \log p(y^i|z^i; \theta), \quad (6)$$

where $z \in \mathbb{Z}$ is latent code and Y represents random variance of the binary categories , $f_c(z) \in \{0, 1\}$. Our goal is to encourage synthetics as a trade-off between both natural creation and man-made artifact categories. When the classifier uncertainty reaches its maximum, $Percept()$ should obtain the optimum. $Percept()$ is described by the following function:

$$Percept(z) = hull(f_c(z)) = -f_c(z)^2 + f_c(z), \quad (7)$$

where *hull* function is a quadratic function that obtains its maximum value at 0.5 possibility, a measure of maximum uncertainty.

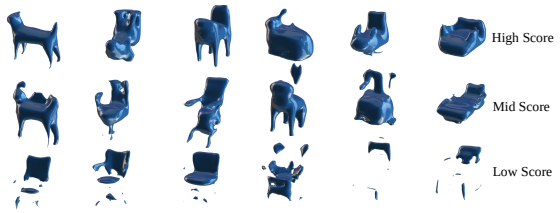

Fig. 9. Effect of scoring function.

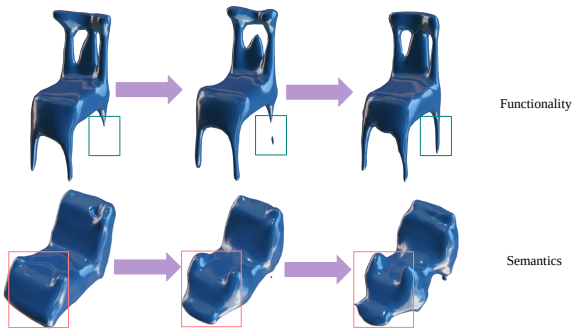

Fig. 10. Effect of local manifold subspace exploration. Two candidates respectively achieved functional and semantic enhancements via first interpretable direction transformation.

The hybrid scoring function contains both classifier perception terms and quality terms:

$$S(z) = Percept(z) + \alpha_1 \phi_{cg}(z) \quad (8)$$

where α_1 is the coefficient of $\phi_{cg}(z)$ terms. $\phi_{cg}(z)$ is a transformation encourage connected components to lower, where is defined as $\phi_{cg}(z) = \frac{1}{1+\text{N}_{cg}(z)}$.

To ensure ideal α_1 and $Percept(z)$ ranges, we ablate two properties of the sampled synthetics. The perception term encourages the shift of the range of generated samples to the OOD area, while the quality function is discrete and concentrated in several fragments of latent space. We finally select the top 10k synthetics with the highest total score and visual effect of the generated geometry. The α, empirically determined to be 0.58, allows control of whether the samples with sub-optimal quality are selected, guaranteeing diversity to some extent. Candidates amounts 10k can be adjusted by users according to the design demands.

Sampling strategy. The method provides a means of latent space optimization for upstream recommend. It maps latent code $\tilde{z}$ from space $\tilde{Z}$ to objective function high score region as a subspace of latent space Z. It is notable that objective function f is evaluated as fewer times as possible and the produced sequence of evaluated points $\mathcal{D}_M \equiv \{x_i, f(x_i)\}_{i=1}^M$. A heuristic sampling method *PrimeSkipSampler* and kernel density estimation is used to form the ground truth point set for the out-of–of-distribution synthesis task.

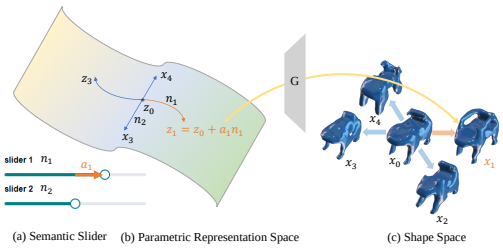

Fig. 11. Introduction of local manifold subspace exploration. A 2-direction example is presented here. The two sub-directions are disentangled, so the user can find 4 kinds of suitable design variants by sliding. Based on initial synthetic x_0, there is several subspace with respect to G decomposition of parametric space as interpretable directions. We can control latent code z_0 via corresponding slider.

Prime skip sampler. The domain, where the high quality samples are located, is narrowed in a convex hull S consisting of whole embedding vectors of the training dataset $\mathcal{D}_{zb} \cap \mathcal{D}_{zd}$. What's more, it is thought that select middle several points from interpolation is an acceptable approach for creative exploration and suitable for a ready-to-use evaluation in convex hull S. If we sample N times for interpolation of each pair of $z_1 \in \mathcal{D}_{zd}$ and $z_2 \in \mathcal{D}_{zb}$ and choose the middle m points in each pair, the samples set $\{\tilde{z}\}$ is as follows:

$$\{\tilde{z}\} = \{\frac{\lambda + \lfloor \frac{N+1}{2} \rfloor}{N} z_1 + (1 - \frac{\lambda + \lfloor \frac{N+1}{2} \rfloor}{N}) z_2 | \lambda = 1, ..., m\}, \quad (9)$$

where N represents the sampling time for interpolation. However, it seems to be a very large number of sampling times for middle m points of interpolation between synthetics. The sample size is $N_{interpolation} = m \times |\mathcal{D}_b||\mathcal{D}_d|$. Aiming to reduce the sample numbers, we find that skipping a prime number during sampling can preserve the algebra structure of interpolations set$\{\tilde{z}\}$. It is a cyclic group of order m while other sampling method in $\{\tilde{z}\}$ is converged to the same structure.

$$\tilde{\{z\}} = \{z_i \in \tilde{z} | i \bmod prime = 0\}. \quad (10)$$

Given t^{th} index $n^{(t)}$ in the cyclic group, we can back calculate (i, j, k) based on following equation:

$$n^{(t)} = t \times prime = (i-1)|\mathcal{D}_{zb}| + (j-1)|\mathcal{D}_{zd}| + k \ (k < m+1). \quad (11)$$

We find corresponding t by sequential enumeration of (i, j, k) and obtain *ExtractBase* function $\phi : \{t \times prime | t \in [0, T-1]\} \rightarrow \{(i, j, k) \in \mathcal{N}^3 | k \in [0, m]\}$

Initial population $Z_I = \{z_k\}_{k=1}^{Y}$ extracted by *Prime Skip Sampler* is shown in Figure 8 d, where each modal represents a category of biologically inspired design. Kernel density estimation(KDE) is used to estimate $p(Z_I)$ from $\hat{Z}_I$: Top 10k samples ranks from $\tilde{\{z\}}$ with bandwidth 0.1. 10k is empirical hyper-parameters and users can adjust further.

Post-process. Post-process are deployed to increase the fidelity of synthetics. We adopted Marching Cube Algorithm [Lorensen and Cline 1987] to extract meshed zero-isosurface from occupation field. Density similarity of triangular lattices allows us to have a uniform criterion for extracting a smooth organic form from these discrete triangular meshes. We therefore used triangulated surface simplification and quadratic smoothing to obtain a smooth surface that meets the designer's expectations. We traded off the resolution of the progressive training, the parameters of the marching cube, and the resolution of sampling from the isosurface. The results of Figure 12 and Figure 13 reveal that the current post-processing strategy leads to the best visual results.

ALGORITHM 1: Pseudocode for *Prime skip sampler.*

Input: Generator G, Objective function f, Latent codes set of nature creations $\mathcal{D}_{zb}$, Latent codes set of man-made artifacts $\mathcal{D}_{zd}$, Max iteration times T, Selection ratio r_s, interpolation points number m.
Output: latent codes set of candidates $\mathcal{D}_{zc}$.

$N_{itp} \leftarrow m|\mathcal{D}_{zb}| \ |\mathcal{D}_{zd}|$;
$prime \leftarrow FindMaxPrime(\lfloor \frac{N_{itp}}{T} \rfloor)$;
$\mathcal{S}_{index} := \{i \in [0, N_{itp}] | i \bmod prime = 0\}$;
$\mathcal{D}_{z\&score} \leftarrow \emptyset$;
for $t \in \mathcal{S}_{index}$: **do**
  $i, j, k = \phi(t)$; $l^{(t)}_{source} = \mathcal{D}_{zb}(i)$; $l^{(t)}_{target} = \mathcal{D}_{zd}(t)$;
  $z^{(t)} \leftarrow l^{(t)}_{source} + \frac{k}{m-1}(l^{(t)}_{target} - l^{(t)}_{source})$;
  $score^{(t)} \leftarrow f(z^{(i)}, G(z^{(i)}))$;
  $\mathcal{D}_{z\&score} \leftarrow \mathcal{D}_{z\&score} \cup \{(z^{(t)}, f(z^{(i)}))\}$;
end
$\mathcal{D}_{zc} \leftarrow Rank(\mathcal{D}_{z\&score}, r_s)$;

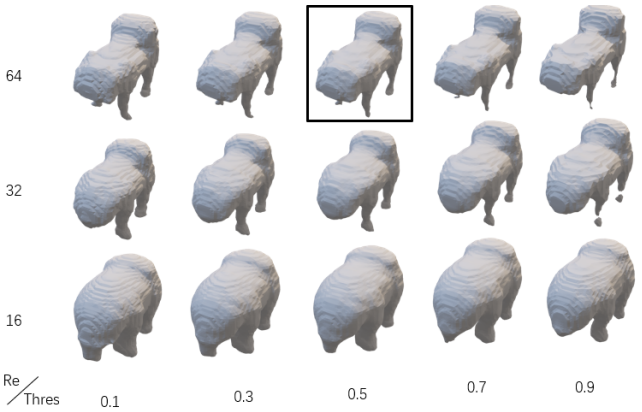

Fig. 12. Ablation study for the relationship between marching cube and progressive training:Thres is the isovalue of marching cube;Re is the resolution in progressive training.

6.3.2 Local manifold subspace exploration. Cold start filters out biologically inspired potential candidates of *high fidelity* and *out-of-distribution*. They help users narrow down their search space. However, there is no guarantee that the filtered candidates will be recognized by users as creative biologically inspired creations. Sampled results will still suffer from local artifacts or feature degradation(see 9). Even for those generators that have both, designers

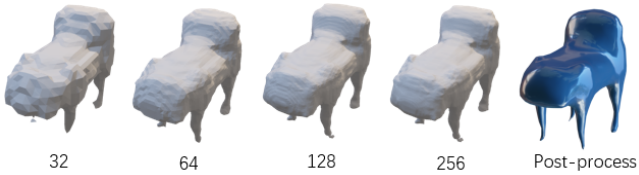

Fig. 13. Ablation study for resolution of implicit representation. The implicit field learned from IMAE have infinite resolution in the cost of memory. The post-process can effectively improve visual effect based on the 64^3 resolution

are eager to explore potential design variants based on these prototypes. Therefore, we hope that synthetics can be fine-tuned to achieve functional and of biologically inspired semantic variants. Our solution is unsupervised based on pretrained generator, which means user can explore local manifold region [Chiu et al. 2020] of certain synthetics via slider interaction(see Figure 10).

Select candidates via projector. Following previous large 3D shape collection exploration work [Averkiou et al. 2014; Chen et al. 2021], we conducts a projector view for visualize the distribution of embedding synthetics via UMap[McInnes et al. 2018]. User will further understanding distribution relationship between synthetics and their reference. Finally, the object x_0 remain to be exploration variants will be selected for local manifold exploration.

Interpretable directions. Exploring interpretable direction (EID) [Shen et al. 2020a] is more suitable as an interactive tool for users to explore potential design variants than as part of an automated pipeline. To address the problem of *feature degradation*, we further consider the interpretable directions as a series local linear subspace of manifold with respect to decoder G. The user is assisted in exploring this local manifold subspace by means of slide bars(see Figure 11).

Considering the avoidance of introducing task-relevant priors and the use of knowledge learned by neural networks, generator-based [Chiu et al. 2020; Shen and Zhou 2021] direction methods are suitable. They focus on the first layer of a generator near the bottleneck. There is a linear transformation $A \in R^{d\times k}$ in the dense layer in front of activation. To extract the k most significant directions $[n_1, n_2, \cdots, n_k]$ of a linear transformation, eigenvectors of the matrix $A^T A$ would achieve the maximum transformation effect and ensure ${n_i}^k$ is distinguishable from others. The latent code received from k^{th} user interaction is that:

$$z^{(k)} = {z_i}^{(k-1)} + \alpha_i n_i, \tag{12}$$

where z_i, α_i, n_i represents the i^{th} dimension of latent code z_i, eigenvalue and eigenvector of $A^T A$ respectively. Finally post-processing enhances the rendering effect through shape decimation and smoothness with smooth shade.

7 INTERFACE

After getting the candidates and determining the semantic direction, an interface is needed to further help the user quickly navigate the candidates and fine-tune them. Figure 14 shows our user-in-loop design interface.

It seems also to be a challenge that select and interpret individual preferences from an unorganized collection of cold start candidates. As an intelligent tool for 3D modeling, an important facet of creativity is human-in-the-loop. The "human" includes not only beginners or nonprofessional general users, but also designers with professional backgrounds. For the average user, they require ready-to-use products and enjoyable exploration through neighborhood discovery and fine-tuning. For professional designers, they tend to explore the intrinsic relationships between various paradigms of biologically inspired design and generative objects. We have summarized their requirements as follows:

- Product traceability problems [Bertolini et al. 2006]:what types of natural creations and man-made artifacts fuse into a given synthetic;
- Product Family Analysis [Jose and Tollenaere 2005]: Which products are of the same family and what are the evolutionary trajectories for a given product;
- Product innovation detection problem [Goldenberg et al. 2002]: How to measure the creative value of synthetics and which products are more creative in terms of generating results.

We designed the user interface to weigh the needs of both user groups. User interface help potential users to explore high-fidelity and diversity synthetics. The solution of our interface for the three previously mentioned requirements is as follows.

- Sampling within one cluster reveal a specific product family. We provide enough thumbnails for users to browse a product family quickly.
- To find which neural creations and man-made artifacts shape features contribute to final synthetics, K training dataset neighborhood of the synthetic serves as a variance of Retrieval task, focusing on retrieving possible biology proper or product elements [Xu et al. 2016].
- Creative synthetics in the realm of design paradigms are modeling to detect outliers from high density regions or big cluster. They are easy to discover in the projector. In addition to the descriptor of implicit autoencoder, the perceptual metric is also taken to differ creative synthetics from common ones.

Our interface provides a projector and 3D viewer for users to explore the design space and view 3D objects, with semantic sliders for user manipulation and a history bar to record saved designs.

Projector. It is mainly used to explore inside the space of candidates and data set associations, similar to shapesynth [Averkiou et al. 2014], The advantage of such a space is that the spatial relationship between the distribution of our candidates and the distribution of the data set can be visualized very well. It can also reveal the internal relationships of the candidates. The user can automatically see that the candidates are showing a varying number of clustering relationships. Our interface also allows the user to highlight the sets of different categories. The user can also zoom in to select the desired item. The selected items change to yellow highlighting. And the selected item is passed to other components, allowing the user to quickly view it and manipulate its 3D shape in several other components. In addition to the exploration method, we also allow

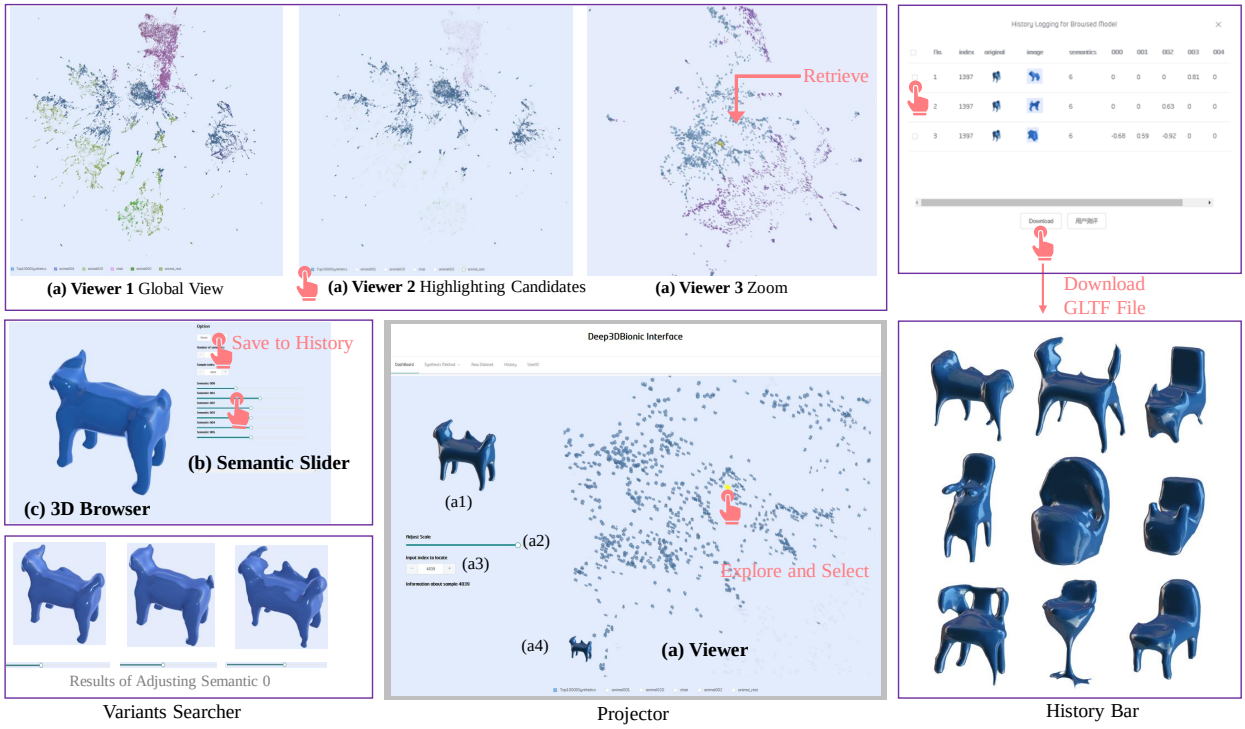

Fig. 14. Our interface for user-in-the-loop design of DeepBionicSyn. Please refer to the demo video for interactive sessions. The middle window contains a projector that allows the user to quick skim the whole latent vectors distribution of training datasets and selected candidates from previous step. Top three windows show three kinds of states of the viewer. Projector is highly interactive for user exploration, such as double click select, select by index(a3), auto camera redirection(Retrieve), category highlight, thumbnails for skimming(a4) and viewing selected candidates(a4), size adjust(a2). Once a candidate is selected, the user can switch to the semantic slider(b) for fine-tuning. The 3D browser(c) allows visualizing real-time change as the slider changes. The post-processing gltf-format 3D model is accessible to rotation ,transformation and zoom. The history bar allows users to retain satisfactory findings for download or subsequent recovery.

the user to quickly redirect the selected object directly based on its history or its ID.

Semantic slider. Once the user has selected the desired synthetic through the projector, we provide a series of semantic sliders based on the Sefa algorithm [Shen and Zhou 2021] to help the user view the local flow shape of the selected object under the synthetic transformation. The sliders represent from high to low the degree of impact on the sliders respectively. According to the subspace search [Chiu et al. 2020], we set the default number of sliders to 6 for efficiency.

3D browser. We provide three layers of views to help users navigate quickly. The first layer tries to load automatically when the user hovers over the projector mouse for a quick view. The second level is a rendered view that specifically shows the selected object. It is used to inform the user which object is currently selected. The third view is the 3D viewer, used to help the user see in real time the changed state of the object after sliding the semantic slider and to allow the user to browse the shape of the 3D object by rotating, scaling, etc.

History. Once the user has selected the object and satisfied with through the projector and semantic slider, the object can be stored in the history by a save button. The stored objects allow the user to download them, access the user research page for evaluation, and go back to recover the state of the operation, including the selected object ID and the corresponding semantic slider adjustments.

8 EVALUATION

We provide a baseline comparison to demonstrate that our approach is better suited to biologically inspired design tasks than other potential alternatives. Then, we explore the performance and utility of our solution in real biologically inspired designs through a user study.

8.1 Baseline comparison

Baseline target. The baseline comparison covers potential alternatives to creative biologically inspired design methods and other OOD synthesis methods as creativity synthetic solver. Dreamfields [Jain et al. 2022], StyleYaYa [Huang et al. 2017], Zoomorphism Design[Duncan et al. 2015] and 3D style transfer methods [Chen et al. 2021; Yifan

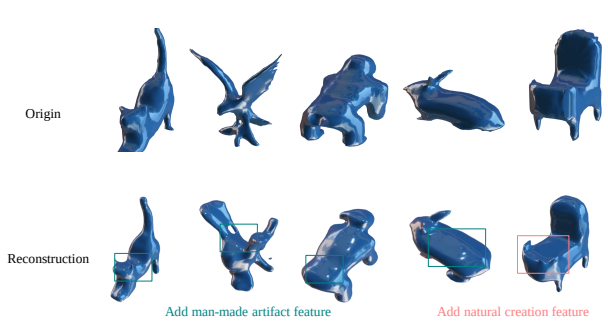

Fig. 15. Semantic entanglement leads to partial training sets with affine value. The first four samples were improved in functionality by sharing the chair feature for the animal category data. The fifth sample has some natural affinity because it shares the animal head feature. This suggests that the entanglement of the common semantics of the data during network training has the potential to bring creativity even to samples from non-OOD regions, contrary to the current trend of pursuing disentanglement of generative model.

et al. 2020] are evaluated to compare the potential geometry blending capability for biologically inspired design with our methods. Random sampling from the l-GAN[Achlioptas et al. 2018] or interpolation method[Wu et al. 2016] serves as the baseline creativity synthetic solver compared with our hybrid score function sampling methods and human-in-the-loop interface.

Qualitative evaluation. As shown in Figure 16, our synthetics are more suitable for creative biologically inspired design tasks than the other baselines. Detail-preserving shape deformation from Neural Cage[Yifan et al. 2020] generate chairs without animal features, violating *category-independent hypothesis*. Decor-GAN [Chen et al. 2021] meets the *synthetic challenge* with respect to local animal features, but fails to address the *modeling challenge* as fidelity is not considered. StyleYaYa provides a more concrete biologically inspired design instead of an organic style biologically inspired design. Due to the lack of materials in the reference data, we only examined StyleYaYa in terms of geometry. The result of Dreamfields is the most creative and visually expressive. However, because it has to satisfy multiple angles of rendering the image at the same time, the animal features are blurred.

The candidate neighbors indicate that our results do not just mimic the reference data(see Figure 20). The use of D-O augmentation allows for a variety of combinations of biologically inspired designs. It is worth noting that our method outputs the common features of a batch of input datasets, while the baseline can only consider a pair of data as input. This means that our approach can be used to extract semantic features that are common to multiple classes of datasets so that even the original training data carry biologically inspired semantics. For example, some animal category reconstruction data also incorporate the semantics of the chair to improve its functionality (see Figure15).

Quantitative evaluation. Quantitative evaluation of the performance is considered in this new task. The metric for *modeling challenge* includes connected component terms $\phi_{cg}(z)$ and shape smoothness M_s in order to measure fidelity and organic style forms. Shape smoothness is computed via mean curvature from the discrete Laplace-Beltrami operator:

$$M_s = \sum_{i=1}^{N} \frac{1}{2} \|\Delta V_i\|_2, \tag{13}$$

where Δ is the discrete Laplace-Beltrami operator and V_i is the i sampled mesh vertex extracted from the zero-isosurface with Marching Cube. N is the number of sampling points, which is 5k following [Yifan et al. 2020].

For the *synthetic challenge*, we attempt to quantify the synthetic bio-inspired value and construct an out-of-distribution score (OOD Score). Generally, if we justify whether a method can generate novel synthetics instead of just imitating the training dataset, we will consider the synthetics set distribution difference with respect to the reference based on the metric of chamfer distance (CD), K nearest neighborhood similarity and Frechet Inception Distance score (FID) [Heusel et al. 2017]. However, some studies have shown that valuable synthetics are not very far from the training dataset distribution but a tradeoff in the parametric representation distance [Elhoseiny and Elfeki 2019; Martindale 1990]. When the distance exceeds this threshold, the sampling results in the latent space lose their task value due to the loss of common features learned in the high probability density region. By regressing this threshold on the scores of the designer's manually designed model, we propose a new metric, the out-of-distribution score (OOD Score). Given a synthetic $x_i \in S_g$ and training dataset $x_j \in S_t$, the OOD score ϕ_{ood} of S_g with respect to S_t is defined as follows:

$$\phi_{ood}(S_g, S_t) = \frac{1}{\sqrt{2}\sigma} e^{-\frac{(D(S_g,S_t)-\hat{u})^2}{2\sigma^2}}, \tag{14}$$

where $\hat{u}$ is the threshold of the optimal design bound. We can rewrite Minimum Matching Distance (MMD) to evaluate the OOD score of S_g with respect to S_r:

$$\phi_{ood}^{mmd}(S_g, S_t) = \frac{1}{\sqrt{2}\sigma} \exp\left(-\frac{\left(\frac{1}{|S_r|}\sum_{x_i \in S_t} \max_{x_j \in S_g} d(x_i, x_j) - \hat{u}\right)^2}{2\sigma^2}\right), \tag{15}$$

where $\hat{u}$ is regressed on global distance $D(S_g^{(k)}, S_t^{(k)})$ of method k and human perception score $\{s_i | 1 \le i \le 4\}$ according to the following equation:

$$\hat{u} = \arg\max_{u} \sum_{k} \left(\frac{1}{\sqrt{2}\sigma} e^{-\frac{\left(D(S_g^{(k)}, S_t^{(k)})-u\right)^2}{2\sigma^2}} \sum_{i} \beta_i s_i^{(k)} + \varepsilon\right), \tag{16}$$

where β_i and ε are coefficients regressed from the human perception score with respect to the metric of two shape $d(x, y)$. The intuitive idea of this construction is to determine the given boundaries based on linear combinations of perceptual scores of real bio-inspired designs from *manual design* and *manual modelling*. For more details, please refer to the supplementary material.

Table 1. The quantitative evaluation comparison to other baseline. KN-MMD, MMD, FID is the closer to *manual modelling* and *manual design* the better. For more clarity, we introduce higher and better OOD score $log\phi_{ood}^{mmd}$ and $log\phi_{ood}^{fid}$. Smoothness M_s and the number of connected components ϕ_{cg} evaluate the quality of synthetics.

	KN-MMD(-)	MMD(-)	FID(-)	$log\phi_{ood}^{mmd}(\uparrow)$	$log\phi_{ood}^{fid}(\uparrow)$	$M_s(\downarrow)$	$\phi_{cg}(\downarrow)$
Our	**3564.09**	**2437.20**	**164.71**	**-7.37**	**-0.39**	**0.03**	2.50
StyleYaYa	3.41	111.77	761	-41.89	-458.82	0.19	1.61
DecorGAN	5.34+E4	5.83+E4	2575.03	-1000.00	-1000.00	1.10	5.26
Neural Cage	58.23	111.07	821.05	-41.92	-560.56	100.12	**1.38**
l-GAN	63.82	67.03	231	-44.47	-0.58	0.75	3.44
Interpolation	14.17	41.73	91.94	-47.24	-11.17	0.43	2.89
Manual modelling	2377.22	1990.67	157.31	1.07	0.58	0.15	1.05
Manual design	2262.80	1538.65	217.81	1.18	0.75	0.15	1.05

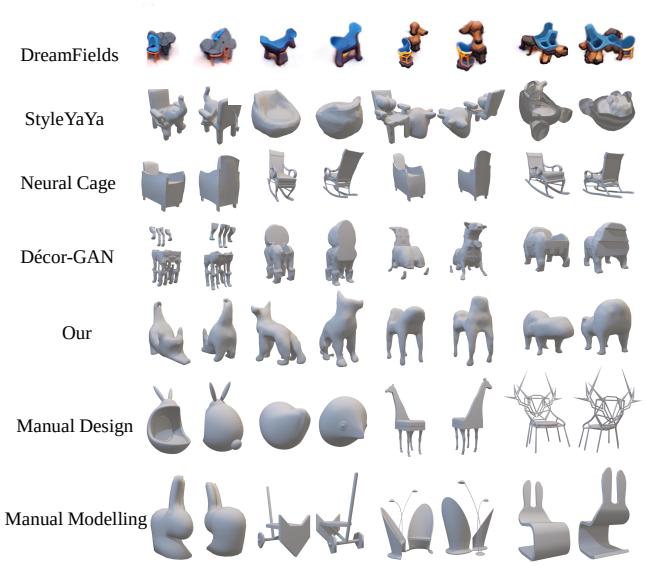

Fig. 16. Comparison with baseline. Each row shows 4 randomly selected shapes. Odd columns represent front view ofbiologically inspired chair while even columns represent back view. The first four rows of shapes are from potential alternatives to our task, the fifth row of shapes are from our method, and the last two rows of shapes are from the designer's manual creation mentioned in the User Study.

8.2 User study

We aim to address two questions from the user studies. The first question is how well our method compares to the work of a human designer. The second question is how much time our method can save compared to manual modeling.

Data. Models generated by DeepBionicSyn were selected and scored by 11 invited users. The users selected 20 of their favorite models through our interface. These data were subject to creator self-evaluation and third-party cross-evaluation. The models from other baselines are also generated and selected by invited volunteers. Because of the lack of presegmentation, the inputs of StyleYaYa were similar to those in our training set from the StyleYaYa segmented dataset, including Stanford cow, rabbit and armchair. DecorGAN and DeepCage were trained with the same animal data as ours and chairs from ShapeNet.

The human designer's biologically inspired design model can be obtained in a more complex manner. To validate the effectiveness of this tool, several professional designers were asked to design biologically inspired models, record the time spent and score the result. As shown in Figure 3, the target for collecting manual biologically inspired design data is divided into the *modeling challenge* and *synthetic challenge*. For the *modeling challenge*, 50 reconstructions were based on existing design concept drawings. Since there are few ready-made 3D models of biologically inspired animal chairs and abundant concept renderings, the designer skipped the concept shape feature fusion stage and modeled the biologically inspired product directly from the existing design picture. The manual models generated in this way are defined as "manual modelling" (see Figure 16 manual modelling). We collected over 1000 images of formwise biologically inspired design from the internet as a reference gallery. A portion of the biologically inspired designs was selected from the gallery based on the salience of natural features, product function, and creative factors. In addition to the existing design products, based on the development of text-driven image generation technology, we also selected some models from DALL·E [Ramesh et al. 2021] with the text prompt in the form of "A in the shape of B". Human designers reconstructed the given images via 3D software and recorded the time spent. After completing the models, the designers scored every model in terms of (a) natural features, (b) creativity, (c) product functionality, and (d) organic style (see Figure 17 for image description). The four terms are defined as *human perception score*.

Regarding the *synthetic challenge*, 50 3D models were independently created by browsing the animal and chair models that were readily available. In the *synthetic challenge*, 3D biologically inspired designs need to be created from scratch without reference. Namely, the designer had the same model as our algorithm training dataset. We recorded the time spent on the design process and the *human perception score* of the design results. The manual models generated in this way are defined as "manual design" (see Figure 16 manual design).

Time cost. We invited individuals to choose and design their favorite biologically inspired design using our interface, and we timed

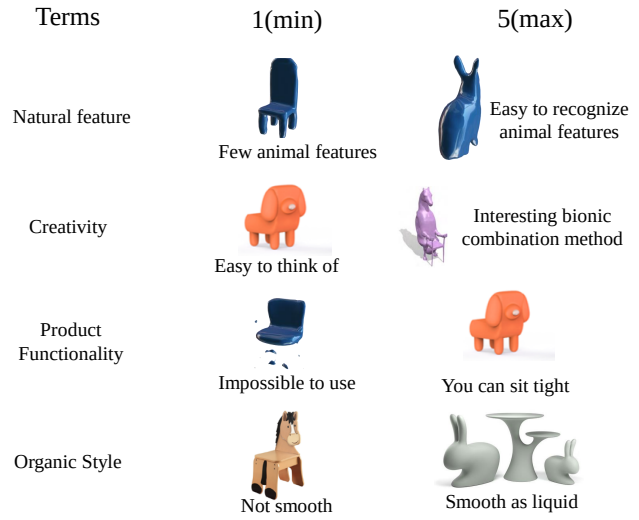

Fig. 17. Scoring standard of user study. Users evaluate biologically inspired shapes following 4 prospective. We provide with referring case and corresponding reason. Scoring object includes our synthetics, manual design and baselines.

each step. As a comparison, we recorded the time spent by the designers when building models based on existing biologically inspired designs (to evaluate the *modeling challenge*), and the time spent improvising after browsing the dataset (to evaluate the *synthetic challenge*). The recorded time included training time t_t and inference time t_i. It is notable that assembly-based methods is no training time, so we define the optimization time as inference time t_i. For manual design for *synthetic challenge*or manual modelling in the *modeling challenge*, the time components are very different. We treated conceptualization outside the modeling software and modeling inside the modeling software as the training time t_t and inference time t_i, respectively. To evaluate the result quality, we recorded the output number as N_g, and the average score of the results in nature features S_{bi}, creativity S_c, product functionality S_{pf} and organic style S_{os} by the invited users. The standard is shown in Figure 17. A more detailed description of each term and implementation environment is described in Appendix III.

Since our method generates a large number of new samples, we should additionally take into account the time it takes for the user to locate a new variant by using a projector and to fine-tune via sliders in the interface. We refer to the former as user browse time t_{ub}, and the latter as user finetune time t_{ut}. Therefore, we calculated the user's exploration time in both processes. We find that user satisfaction with the generated objects is significantly increased by a certain degree of customization of interactive exploration.

Scoring. The *human perception score* includes (a) natural features, (b) creativity, (c) product functionality and (d) organic style (see Figure 17 for image description):

(1) Natural features indicate the degree of visual similarity between the current design and the animal. If the animal reference can be recognized, the highest score will be awarded.

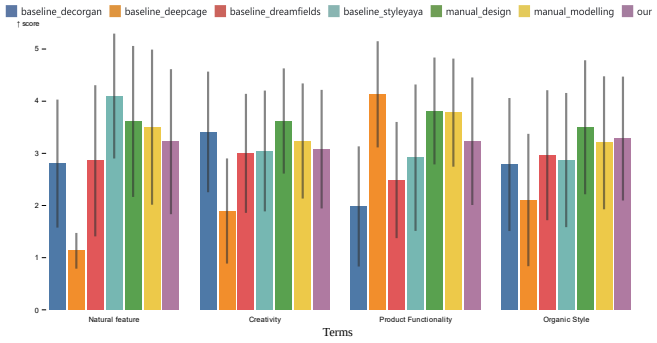

Fig. 18. Average score for *human perception score* in user study.

(2) Creativity indicates whether the model is aesthetically pleasing or whether the way the chair and animal features are combined is more interesting. Creativity is also used to evaluate whether the algorithm solves the feature degradation problem.
(3) Functionality is used to evaluate whether the design as a chair is structurally reasonable and can be 3D printed for manufacturing after fine-tuning.
(4) The organic style emphasizes harmony between human habitation and the natural world[Wikipedia 2022]. In this work, we emphasize an abstract and smooth stylistic form.

Case result. Invited professional designers completed the following tasks via our interface. First, they became familiar with the latent space with the help of embedding point space relationships and some representative synthetics. Second, they searched the local manifold subspace to deform selected synthetics with several sliders. Figure 19 shows the case results. The time records t_{ub} and t_{ut} in Table 2 illustrates that the user can select desired candidates in one minute and finetune them in two minutes. It demonstrates that our work can be used to guide users to create satisfactory organic biologically inspired designs in a suitable time frame. Because of the interface guide, users can spend less time designing the desired effect they want. When we cross-scored the samples obtained by browsing only and those obtained by finetuning to third-party users, the results also showed that it was worthwhile to spend some time fine-tuning the result with the slider in exchange for higher-quality biologically inspired design results.

Review. Users were generally satisfied with the interface and the results of our method, including the richness of candidate samples displayed in the projector and the ease of viewing the samples for the current biologically inspired design reference. The high-level adjustment provided by the semantic slider bar may be more convenient than using the modeling software. However, users also suggested that the changes brought by the semantic slider adjustment are difficult to control and some reference examples before adjustment need to be given. This problem was somewhat alleviated after we quickly provided a rendering of each slider adjusted by 0.5 according to the positive and negative values. In the future, we hope to make

Table 2. The time spent and human perception score for our method, four baseline methods and two kinds of biologically inspired designs created by professional designers. The time spent illustrates the efficiency of our algorithm and interface. The human perception score indicates that our approach is nearest of human designs in the creative biologically inspired design tasks with less time spent. We highlight the top two methods whose S_{bi}, S_c and S_{pf} scores are closest to the manual data.

Method	t_t(per shape)	t_i(per shape)	t_{ub}	t_{ut}	N_g	S_{bi}	S_c	S_{pf}	S_{os}
Our	24E-04h	0.33s	37.97	93.79	batch	**3.38**	**3.34**	**3.47**	**3.57**
Dreamfields	72h	60s	-	-	single	2.38	2.92	2.38	2.86
Neural Cage	8.85E-04h	0.95s	-	-	batch	1.04	1.77	**4.27**	2.23
DecorGAN	17E-04h	0.42s	-	-	batch	2.69	**3.66**	1.88	3.00
Styleyaya	-	0.24h	-	-	single	**3.90**	3.06	2.69	2.78
Manual design	0.31h	1.68h	-	-	single	3.65	3.76	3.90	3.60
Manual modelling	-	1.66h	-	-	single	3.36	3.35	3.88	3.23

the semantic changes brought by the sliders consistent for each candidate.

Scoring result. The human perception scores of over 2.7k samples (see Figure 18) were collected by 20 third-party invited users. The users were told to read Figure 17 in advance and score each sample. Most users were university students majoring in computer science or design. The remaining users were experts in related fields. See the Appendix for specific questionnaire data and demographic information. The highest rating among the four items is manual design for the *synthetic challenge*, followed by manual modelling for *modeling challenge*. This means that the biologically inspired design considering the *synthetic challenge* in the creation process is indeed of higher organic biologically inspired value. Thus, our approach is comparable to human work in all human perception scores, while other baselines have strengths in only one of the terms and significant weaknesses elsewhere. StyleYaYa, which is based on presegmented and assembled components, has a higher natural features score due to the realistic component image, but is deficient in terms of creativity. The two style transfer approaches have completely opposite advantages and disadvantages. DecorGAN is more innovative, but less functional because it does not take into account the breakage problems associated with detailed animal features, while DeepCage is less innovative and more functional because cages cannot integrate detailed animal features into the chair.

8.3 Ablation study

We conducted ablation studies to validate each module related to the biologically inspired design results, i.e., data augmentation, score function in the cold start and postprocessing. To ablate the effect of the creativity synthetic solver, we replaced this module with l-GAN and random interpolation. Finally, we retained the reconstruction as a control group. The evaluation metrics include MMD and quality score ϕ_{cg} and M_s.

The ablation study of our method (see Table 3) revealed that the creativity synthetic solvercan significantly improve the quality of synthetics in the OOD region. Figure 21 quantitatively illustrates the effects brought about by our individual components. The interpolation method is prone to fragmentation problems due to the lack of quality constraints on the hybrid objective function. The D-O and P-O methods can alleviate the underfitting and overfitting problems respectively. These two issues are critical to the latent space sampling results.

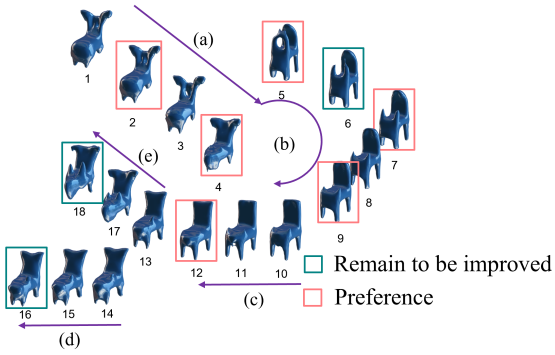

Fig. 19. Effect of semantic direction. We invite volunteers to explore the potential semantic directions through the slider bar. (a-f) shows a kind of semantic transform designers recognize respectively. Participants successfully identified their preferred results in the process and adjusted the design they felt could be improved through the slider. More detailed semantic annotation are stated in Appendix.

8.4 Limitation

Our method does not always generate biologically inspired form with high recognizability (e.g., Figure 22). One straightforward method to alleviate this problem is to decrease the ratio of selected samples in cold start.

9 APPLICATION

The biologically inspired design results can be used to produce children's furniture and sculpture design for scenes. It expresses the tendency to live in harmony with nature and achieve sustainable development.

The goal of generating objects for children's scenes is to create interesting and safe objects. To achieve this, we need to generate a diverse range of samples and carefully control the value of the sampling objective function to produce organic and smooth results that avoid sharp edges. These adjustments ensure that the initial distribution of cold start candidates presented to the user in the interface

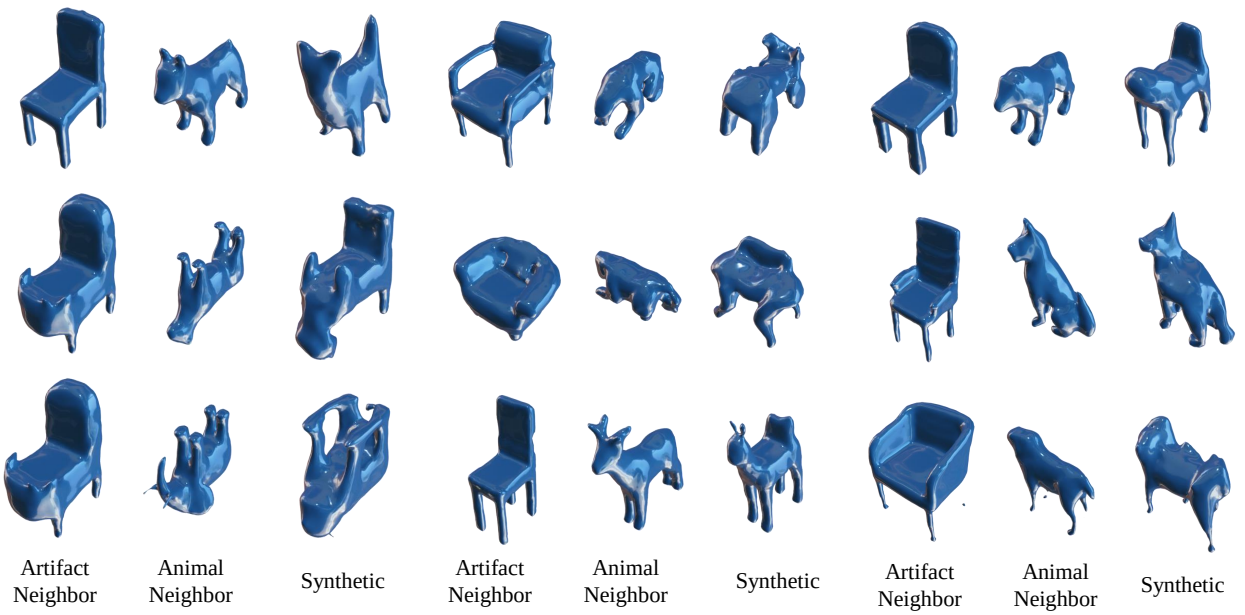

Fig. 20. The neighborhood of synthetics. We explored the training dataset latent codes with the nearest Euclidean distance to the given synthetics in the latent space. Each of the three columns from left to right represents the nearest man-made artifacts, natural creations and synthetics itself respectively. The results show that our approach does not simply assemble the components of the reference shape but rather abstracts the morphology to form organic results.

Table 3. Ablation study of our methods. We first tested our pipeline without postprocessing and design-oriented and performance-oriented augmentation strategies. Then, we generated synthetics via l-GAN and interpolation instead of our proposed creativity synthetic solver. As a control group, we also tested direct reconstruction. KN-MMD is the MMD of the nearest 5 neighbors scaled by 10^5 with the Chamfer distance.

	KN-MMD(↑)	R-MMD(↓)	MMD(↑)	M_s(↓)	ϕ_{cg}(↓)
Our	**3564.09**	11.48	**2437.20**	**0.03**	2.50
W/O postprocess	32.41	11.48	18.93	0.64	1.42
W/O D-O	217.42	**4.77**	209.27	0.13	**1.35**
W/O P-O	49.51	5.51	10.62	0.57	1.91
l-GAN	67.03	-	63.82	1.50	3.44
Interpolation	41.73	-	14.17	0.43	2.89
Reconstruction	12.73	-	11.48	0.64	1.97

is appropriate. As an example, Figure 23 (a) and (c) show a scenario that is suitable for this application. Using the interface, designers can search for candidates related to friendly animals and interesting chairs. In the projection of the latent space, several major categories of images can be observed. In this case, the users selected the cat chair, the round dog head chair, and the reclining elephant chair, as these designs better preserved the shape of the original biologically inspired creatures. In addition, children's furniture needs to be functional and safe. We found that specific combinations are particularly effective in producing solid and reliable chairs. For example, the network has learned a priori knowledge that chairs and animals both have four legs for support, which creates a stable structure.

The modern art of park sculptures requires a greater degree of diversity, and we have found that combining different directions has a significant impact on this target scene. By merging the side of a chair with the shape of an animal through D-O augmentation, we are able to create fashionable and organic designs (see Figure 23 (d)). Additionally, to achieve a diverse set of designs, we often explore the distributions of synthetics with lower values of the hybrid function, or regions of small distribution. This presents a challenge in terms of quality, but we can use fine-tuning based on the quality term to automatically find variants with one connected component, allowing us to achieve functionality while preserving the original artistic form. The designers have also creatively used the platform on the back of a cat-related synthetic object to design a table (see Figure 23 (b)).

10 CONCLUSION AND FUTURE WORK

In this paper, an automated framework of creative biologically inspired design framework is presented. We design a two-stage approach by first providing a parametric representation and then

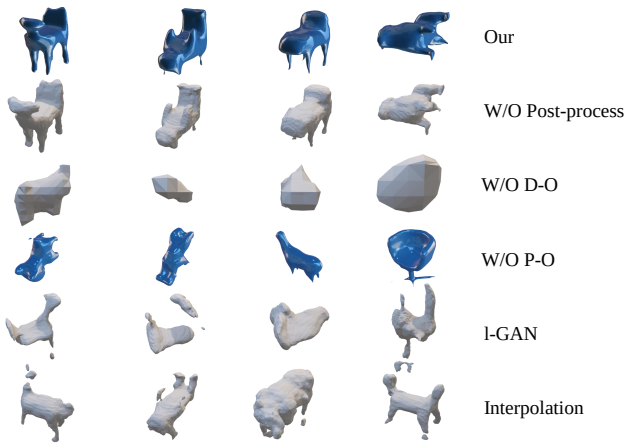

Fig. 21. The ablation results for each of our component.

(a) Less artifacts feature (b) Less natural creations feature (c) Unlike both categories

Fig. 22. Failure case for DeepBionicSyn. Samples with low OOD scores tend to be too close to the original data, leading to feature degradation from one categories of input dataset thus reducing the biologically inspired value. The third problem is caused by naive quality assessment function. Even if the quality score is high, some candidates may still have artifacts. Three problems can be alleviated by improving the hybrid objective function.

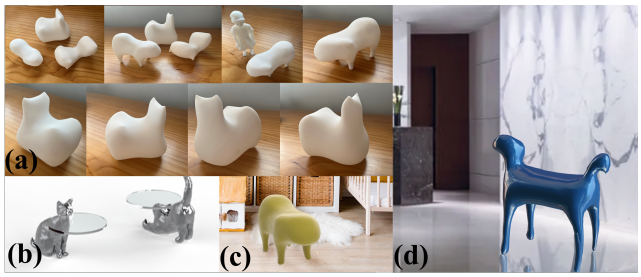

Fig. 23. Application examples of generated biologically inspired designs. (a) 3D print results of candidates preferring by designers. (b) Cat tables were created as a biologically inspired design. (c) Since it has an eco-friendly appearance, organic style bio-inspired furniture created with our method is available to enhance the life of children. (d) Our algorithms can produce more inventive forms for designing urban landscapes.

extracting generators with biologically inspired value from the parametric representation space through a creativity synthetic solver. We compare our approach to other competitors and demonstrate its effectiveness in biologically inspired design tasks. We also conduct a user study to evaluate the performance and utility of our solution in real-world scenarios.

Our future work includes multimodal and more fine-grained biologically inspired designs. *Multimodal methods.*Deep implicit representation overtakes segmented partwise representation, which is thought to be a kind of future form fit-and-diverse form [Xu et al. 2012]. However, we retain geometric synthesis instead of a high-quality textured shape. A multimodal learning framework may contribute to more biologically inspired design possibilities. In addition to recent domain-specific textured representation implicit models [Gao et al. 2021], neural rendering-based methods such as NeRF [Mildenhall et al. 2020] make it possible to generate whole scenes. Existing zero-shot text-prompt NeRF [Jain et al. 2022] will bring a promising direction. *Various grained biologically inspired designs.* Despite the fact that an out-of-distribution area covers most of organic biologically inspired designs, we find that our implicit generative model guarantees a middle-grained shape blend. Interestingly, recent study [Vinker et al. 2022] showed that semantic-aware shape fusion at various granularities seems to be possible with the help of CLIP (contrastive-language-image-pretraining) [Radford et al. 2021].

REFERENCES

Panos Achlioptas, Olga Diamanti, Ioannis Mitliagkas, and Leonidas Guibas. 2018. Learning representations and generative models for 3d point clouds. In *International conference on machine learning*. PMLR, 40–49.

Ramtin Attar, Robert Aish, Jos Stam, Duncan Brinsmead, Alex Tessier, Michael Glueck, and Azam Khan. 2010. Embedded rationality: A unified simulation framework for interactive form finding. *International journal of architectural computing* 8, 4 (2010), 399–418.

Melinos Averkiou, Vladimir G Kim, Youyi Zheng, and Niloy J Mitra. 2014. Shapesynth: Parameterizing model collections for coupled shape exploration and synthesis. In *Computer Graphics Forum*, Vol. 33. Wiley Online Library, 125–134.

Massimo Bertolini, Maurizio Bevilacqua, and Roberto Massini. 2006. FMECA approach to product traceability in the food industry. *Food control* 17, 2 (2006), 137–145.

Ardavan Bidgoli and Pedro Veloso. 2019. Deepcloud. the application of a data-driven, generative model in design. *arXiv preprint arXiv:1904.01083* (2019).

Angel X Chang, Thomas Funkhouser, Leonidas Guibas, Pat Hanrahan, Qixing Huang, Zimo Li, Silvio Savarese, Manolis Savva, Shuran Song, Hao Su, et al. 2015. Shapenet: An information-rich 3d model repository. *arXiv preprint arXiv:1512.03012* (2015).

Siddhartha Chaudhuri, Evangelos Kalogerakis, Stephen Giguere, and Thomas Funkhouser. 2013. Attribit: content creation with semantic attributes. In *Proceedings of the 26th annual ACM symposium on User interface software and technology*. 193–202.

Siddhartha Chaudhuri and Vladlen Koltun. 2010. Data-driven suggestions for creativity support in 3d modeling. In *ACM SIGGRAPH Asia 2010 papers*. 1–10.

Wei Chen and Faez Ahmed. 2020. PaDGAN: A Generative Adversarial Network for Performance Augmented Diverse Designs. In *International Design Engineering Technical Conferences and Computers and Information in Engineering Conference*, Vol. 84003. American Society of Mechanical Engineers, V11AT11A010.

Zhiqin Chen, Vladimir G Kim, Matthew Fisher, Noam Aigerman, Hao Zhang, and Siddhartha Chaudhuri. 2021. DECOR-GAN: 3D Shape Detailization by Conditional Refinement. In *Proceedings of the IEEE/CVF Conference on Computer Vision and Pattern Recognition*. 15740–15749.

Zhiqin Chen and Hao Zhang. 2019. Learning implicit fields for generative shape modeling. In *Proceedings of the IEEE Conference on Computer Vision and Pattern Recognition*. 5939–5948.

Chia-Hsing Chiu, Yuki Koyama, Yu-Chi Lai, Takeo Igarashi, and Yonghao Yue. 2020. Human-in-the-loop differential subspace search in high-dimensional latent space. *ACM Transactions on Graphics (TOG)* 39, 4 (2020), 85–1.

Alexey Dosovitskiy, Jost Tobias Springenberg, and Thomas Brox. 2015. Learning to generate chairs with convolutional neural networks. In *Proceedings of the IEEE conference on computer vision and pattern recognition*. 1538–1546.

Noah Duncan, Lap-Fai Yu, Sai-Kit Yeung, and Demetri Terzopoulos. 2015. Zoomorphic design. *ACM Transactions on Graphics (TOG)* 34, 4 (2015), 1–13.

Ahmed Elgammal, Bingchen Liu, Mohamed Elhoseiny, and Marian Mazzone. 2017. CAN: Creative adversarial networks generating "Art" by learning about styles and deviating from style norms. In *8th International Conference on Computational Creativity, ICCC 2017*. Georgia Institute of Technology.

Mohamed Elhoseiny and Mohamed Elfeki. 2019. Creativity inspired zero-shot learning. In *Proceedings of the IEEE/CVF International Conference on Computer Vision*. 5784–5793.

Lin Gao, Tong Wu, Yu-Jie Yuan, Ming-Xian Lin, Yu-Kun Lai, and Hao Zhang. 2021. Tm-net: Deep generative networks for textured meshes. *ACM Transactions on Graphics (TOG)* 40, 6 (2021), 1–15.

Jacob Goldenberg, David Mazursky, and Goldenberg Jacob. 2002. *Creativity in product innovation*. Cambridge University Press.

Xuekun Guo, Juncong Lin, Kai Xu, and Xiaogang Jin. 2014. Creature grammar for creative modeling of 3D monsters. *Graphical Models* 76, 5 (2014), 376–389.

Erik Härkönen, Aaron Hertzman, Jaakko Lehtinen, and Sylvain Paris. 2020. GANSpace: Discovering Interpretable GAN controls. In *IEEE Conference on Neural Information Processing Systems;*.

Martin Heusel, Hubert Ramsauer, Thomas Unterthiner, Bernhard Nessler, and Sepp Hochreiter. 2017. Gans trained by a two time-scale update rule converge to a local nash equilibrium. *Advances in neural information processing systems* 30 (2017).

Steven Skov Holt, Mara Holt Skov, Phil Patton, and Bruce Sterling. 2005. *Blobjects and beyond: The new fluidity in design*. Chronicle Books.

Yi-Jheng Huang, Wen-Chieh Lin, I-Cheng Yeh, and Tong-Yee Lee. 2017. Geometric and textural blending for 3d model stylization. *IEEE transactions on visualization and computer graphics* 24, 2 (2017), 1114–1126.

Ajay Jain, Ben Mildenhall, Jonathan T. Barron, Pieter Abbeel, and Ben Poole. 2022. Zero-Shot Text-Guided Object Generation with Dream Fields. (2022).

Alberto Jose and Michel Tollenaere. 2005. Modular and platform methods for product family design: literature analysis. *Journal of Intelligent manufacturing* 16, 3 (2005), 371–390.

Evangelos Kalogerakis, Siddhartha Chaudhuri, Daphne Koller, and Vladlen Koltun. 2012. A probabilistic model for component-based shape synthesis. *Acm Transactions on Graphics (TOG)* 31, 4 (2012), 1–11.

Tero Karras, Samuli Laine, and Timo Aila. 2019. A style-based generator architecture for generative adversarial networks. In *Proceedings of the IEEE/CVF Conference on Computer Vision and Pattern Recognition*. 4401–4410.

Stephen R Kellert, Judith Heerwagen, and Martin Mador. 2011. *Biophilic design: the theory, science and practice of bringing buildings to life*. John Wiley & Sons.

William E Lorensen and Harvey E Cline. 1987. Marching cubes: A high resolution 3D surface construction algorithm. *ACM siggraph computer graphics* 21, 4 (1987), 163–169.

Joe Marks, Brad Andalman, Paul A Beardsley, William Freeman, Sarah Gibson, Jessica Hodgins, Thomas Kang, Brian Mirtich, Hanspeter Pfister, Wheeler Ruml, et al. 1997. Design galleries: A general approach to setting parameters for computer graphics and animation. In *Proceedings of the 24th annual conference on Computer graphics and interactive techniques*. 389–400.

Colin Martindale. 1990. *The clockwork muse: The predictability of artistic change*. Basic Books.

Justin Matejka, Michael Glueck, Erin Bradner, Ali Hashemi, Tovi Grossman, and George Fitzmaurice. 2018. Dream lens: Exploration and visualization of large-scale generative design datasets. In *Proceedings of the 2018 CHI conference on human factors in computing systems*. 1–12.

Leland McInnes, John Healy, and James Melville. 2018. Umap: Uniform manifold approximation and projection for dimension reduction. *arXiv preprint arXiv:1802.03426* (2018).

Lars Mescheder, Michael Oechsle, Michael Niemeyer, Sebastian Nowozin, and Andreas Geiger. 2019. Occupancy networks: Learning 3d reconstruction in function space. In *Proceedings of the IEEE Conference on Computer Vision and Pattern Recognition*. 4460–4470.

Ben Mildenhall, Pratul P. Srinivasan, Matthew Tancik, Jonathan T. Barron, Ravi Ramamoorthi, and Ren Ng. 2020. NeRF: Representing Scenes as Neural Radiance Fields for View Synthesis. In *ECCV*.

Fakir S. Nooruddin and Greg Turk. 2003. Simplification and repair of polygonal models using volumetric techniques. *IEEE Transactions on Visualization and Computer Graphics* 9, 2 (2003), 191–205.

Sangeun Oh, Yongsu Jung, Seongsin Kim, Ikjin Lee, and Namwoo Kang. 2019. Deep generative design: Integration of topology optimization and generative models. *Journal of Mechanical Design* 141, 11 (2019).

Jeong Joon Park, Peter Florence, Julian Straub, Richard Newcombe, and Steven Lovegrove. 2019. Deepsdf: Learning continuous signed distance functions for shape representation. In *Proceedings of the IEEE Conference on Computer Vision and Pattern Recognition*. 165–174.

Alec Radford, Jong Wook Kim, Chris Hallacy, Aditya Ramesh, Gabriel Goh, Sandhini Agarwal, Girish Sastry, Amanda Askell, Pamela Mishkin, Jack Clark, et al. 2021. Learning transferable visual models from natural language supervision. In *International Conference on Machine Learning*. PMLR, 8748–8763.

Aditya Ramesh, Mikhail Pavlov, Gabriel Goh, Scott Gray, Chelsea Voss, Alec Radford, Mark Chen, and Ilya Sutskever. 2021. Zero-shot text-to-image generation. *arXiv preprint arXiv:2102.12092* (2021).

Othman Sbai, Mohamed Elhoseiny, Antoine Bordes, Yann LeCun, and Camille Couprie. 2018. Design: Design inspiration from generative networks. In *Proceedings of the European Conference on Computer Vision (ECCV) Workshops*. 0–0.

Nadav Schor, Oren Katzir, Hao Zhang, and Daniel Cohen-Or. 2019. Componet: Learning to generate the unseen by part synthesis and composition. In *Proceedings of the IEEE/CVF International Conference on Computer Vision*. 8759–8768.

Yujun Shen, Jinjin Gu, Xiaoou Tang, and Bolei Zhou. 2020a. Interpreting the latent space of gans for semantic face editing. In *Proceedings of the IEEE/CVF Conference on Computer Vision and Pattern Recognition*. 9243–9252.

Yujun Shen, Ceyuan Yang, Xiaoou Tang, and Bolei Zhou. 2020b. Interfacegan: Interpreting the disentangled face representation learned by gans. *IEEE transactions on pattern analysis and machine intelligence* (2020).

Yujun Shen and Bolei Zhou. 2021. Closed-Form Factorization of Latent Semantics in GANs. In *CVPR*.

Dule Shu, James Cunningham, Gary Michael Stump, Simon W Miller, Michael Andrew Yukish, Timothy W Simpson, and Conrad S Tucker. 2020. 3D Design Using Generative Adversarial Networks and Physics-Based Validation. *Journal of Mechanical Design, Transactions of the ASME* 142, 7 (2020), 071701.

Nobuyuki Umetani. 2017. Exploring generative 3d shapes using autoencoder networks. In *SIGGRAPH Asia 2017 Technical Briefs*. 1–4.

Yael Vinker, Ehsan Pajouheshgar, Jessica Y. Bo, Roman C. Bachmann, Amit Bermano, Daniel Cohen-Or, Amir Zamir, and Ariel Shamir. 2022. CLIPasso: Semantically-Aware Abstract Object Sketching. *ACM Transactions on Graphics (SIGGRAPH Proceedings)* 41, 4 (2022), Article 86, 1–11.

Yulin Wang, Gao Huang, Shiji Song, Xuran Pan, Yitong Xia, and Cheng Wu. 2021. Regularizing deep networks with semantic data augmentation. *IEEE Transactions on Pattern Analysis and Machine Intelligence* (2021).

Wikipedia. 2022. Organic architecture — Wikipedia, The Free Encyclopedia. http://en.wikipedia.org/w/index.php?title=Organic%20architecture&oldid=1089962653. [Online; accessed 14-October-2022].

Jiajun Wu, Chengkai Zhang, Tianfan Xue, William T Freeman, and Joshua B Tenenbaum. 2016. Learning a probabilistic latent space of object shapes via 3d generative-adversarial modeling. *arXiv preprint arXiv:1610.07584* (2016).

Weihao Xia, Yulun Zhang, Yujiu Yang, Jing-Hao Xue, Bolei Zhou, and Ming-Hsuan Yang. 2021. Gan inversion: A survey. *arXiv preprint arXiv:2101.05278* (2021).

Kai Xu, Vladimir G Kim, Qixing Huang, Niloy Mitra, and Evangelos Kalogerakis. 2016. Data-driven shape analysis and processing. In *SIGGRAPH ASIA 2016 Courses*. 1–38.

Kai Xu, Hao Zhang, Daniel Cohen-Or, and Baoquan Chen. 2012. Fit and diverse: Set evolution for inspiring 3d shape galleries. *ACM Transactions on Graphics (TOG)* 31, 4 (2012), 1–10.

Zhijin Yang, Pengfei Xu, Hongbo Fu, and Hui Huang. 2021. WireRoom: model-guided explorative design of abstract wire art. *ACM Transactions on Graphics (TOG)* 40, 4 (2021), 1–13.

Wang Yifan, Noam Aigerman, Vladimir G Kim, Siddhartha Chaudhuri, and Olga Sorkine-Hornung. 2020. Neural cages for detail-preserving 3d deformations. In *Proceedings of the IEEE/CVF Conference on Computer Vision and Pattern Recognition*. 75–83.

Simiao Yu, Hao Dong, Pan Wang, Chao Wu, and Yike Guo. 2019. Generative Creativity: Adversarial Learning for bionically inspired Design. In *International Conference on Artificial Neural Networks*. Springer, 525–536.

Yonghao Yue, Yuki Koyama, Issei Sato, and Takeo Igarashi. 2021. User Interfaces for High-Dimensional Design Problems: From Theories to Implementations. In *ACM SIGGRAPH 2021 Courses (SIGGRAPH '21)*. Association for Computing Machinery, New York, NY, USA, Article 11, 34 pages. https://doi.org/10.1145/3450508.3464551

Silvia Zuffi, Angjoo Kanazawa, David W Jacobs, and Michael J Black. 2017. 3D menagerie: Modeling the 3D shape and pose of animals. In *Proceedings of the IEEE conference on computer vision and pattern recognition*. 6365–6373.